國　立　交　通　大　學

電機與控制工程學系

碩　士　論　文

應用卡爾曼濾波器在 GPS 接收器的追蹤技術

A NEW TRACKING TECHNIQUE USING KALMAN FILTER FOR GPS RECEIVER

研 究 生：李浩緯

指導教授：鄭木火 博士

中 華 民 國 九 十 五 年 七 月

應用卡爾曼濾波器在 GPS 接收器的追蹤技術

A NEW TRACKING TECHNIQUE USING KALMAN FILTER FOR GPS RECEIVER

研 究 生：李浩緯　　Student : Hao-Wei Li

指導教授：鄭木火 博士　　Advisor : Dr. Mu-Huo Cheng

國 立 交 通 大 學

電機與控制工程學系

碩士論文

A Thesis

Submitted to Department of Electrical and Control Engineering

College of Electrical and Computer Engineering

National Chiao Tung University

In Partial Fulfillment of the Requirements

For the Degree of

Master of Science

In

Electronics Engineering

June 2006

Hsinchu, Taiwan, Republic of China

中 華 民 國 九 十 五 年 七 月

應用卡爾曼濾波器在 GPS 接收器的追蹤技術

研究生: 李浩緯　　指導教授:鄭木火 博士

國立交通大學電機與控制工程學系

摘要

訊號擷取在全球定位系統(GPS)接收器中的目的是為了追蹤估測偽隨機碼(Pseudo-Random Number, PRN)的延遲時間和都普勒頻率。追蹤方法利用延遲/提早的方法並且經由一個擁有迴路濾波器的閉迴路系統來實現。而迴路濾波器往往使用一個比例積分(Proportional-Integral, PI)濾波器。使用比例積分濾波器的參數需要依賴經驗來調整，追蹤效能隨著比例積分濾波器參數的選擇而變動。本篇論文把估測偽隨機的延遲時間和都普勒頻率的追蹤設定為觀察者設計的問題，如此擴張卡爾曼濾波器被用來實現這個觀察者。估測偽隨機的延遲時間的追蹤可用數位延遲鎖相迴路(digital delayed-locked loop, DDLL)來實現，並且設定為一個非線性觀察者問題，如此擴張卡爾曼濾波器可被用來估測延遲時間。都普勒頻率的追蹤可用數位鎖相迴路(digital phase-locked loop, DPLL)來實現，並且設定為一個線性觀察者問題，因此卡爾曼濾波器可當作是觀察者。此方法不但減輕設計濾波器參數的負擔並且是一個快速追蹤的演算法。使用電腦模擬來驗證本論文所題方法之優越性。

關鍵詞：全球定位系統，偽隨機碼，卡爾曼濾波器

A NEW TRACKING TECHNIQUE USING ALMAN FILTER FOR GPS RECEIVER

Student: Hao-Wei Li Advisor: Dr. Mu-Huo Cheng

Institute of Electrical and Control Engineering
National Chiao Tung University

Abstract

The goal of signal tracking in GPS receiver is to track the Pseudo-Random Number (PRN) code delay and the Doppler frequency. The tracking methods are performed using early-late method via a closed loop with a loop filter. The PI is commonly used to realize the loop filter; The PI parameters are empirically determined. The tracking performance varies with the choice of PI parameters. This thesis configures the tracking of PRN code delay and Doppler frequency as problems of observer design, such that the extended Kalman filter (EKF) and Kalman filter (KF) algorithm are applied realize the observers. The tracking of PRN code delay which is realized by a digital delay-locked loop is configured as a nonlinear observer problem such that the EKF can be used to estimate the delay, while the tracking of the Doppler frequency realized by a digital phase-locked loop, is configured as a linear observer problem, hence the KF can be used as the observer. This approach not only alleviates the burden of designing PI parameters but also obtain a fast tracking algorithm. Computer simulations are also performed to demonstrate the advantages of our proposed method.

Keywords：GPS, PRN, Kalman filter

誌謝

此論文能順利完成，要特別真誠地感謝我的指導教授鄭木火老師，在短短的兩年研究生涯中，在研究上循循善誘，一次又一次的幫助我解決困難，並且讓我學習分析問題並加以解決的能力，因此無論在待人接物處事以及治學的嚴謹態度，均使我獲益良多。本論文付梓之際，對於耐心傳道授業的老師至上最誠摯的謝意。

感謝在電控所 914 實驗室裡所提供完備的研究資源。承蒙學姐佩樺、學長嘉富的提攜與照顧，在研究與生活上都能順利解決問題。而實驗室一起打拼的同伴信良、啟峰、俊維還有室友崇諺、鴻志、人中在課業上的砥礪以及生活上的互相鼓勵與幫助，讓我在忙碌的研究生活中依然保持愉悅的心情。也感謝學弟衍禎、佳華、嘉明，在你們的幫助下，論文得以順利得完成。感謝阿妃阿姨在研究所兩年日子的照顧。更要感謝高中到研究所得同隊好友邱子長，以及在棒球隊裡的教練、學長、學弟們，讓我的學生生活多采多姿。

最後，感謝我的家人，溫暖的家讓我可以無後顧之憂得汲取知識，努力於我的課業上，順利完成我的學業，並做好面對下一個階段挑戰的準備。

Contents

List of Figures

List of Tables

Chapter 1

INTRODUCTION

1.1 Introduction

Global Positioning System (GPS) navigation receiver must acquire and track four GPS satellites at least. In order to track and decode the navigation data from the received signal, an acquisition process must detect the presence of the GPS signal. Once the GPS signal is detected, the coarse PRN code delay and Doppler frequency can be obtained and passed to the tracking program. The function of the tracking program is to demodulate the PRN signal and to obtain the navigation data. If the initial code delay and the Doppler frequency from the acquisition process are not accurate enough, the tracking program must make more effort to achieve the fine resolution of the code delay and Doppler frequency. The conventional tracking process using a early-late method via a closed loop with a loop filter. In this thesis, we choose the Kalman filter to realize the loop filter. According to the DDLL and DPLL model [3], the message and measurement model of the Kalman filter can be established [6]. The Kalman filter has the advantage of easy design and the high reliability to achieve the fine performance. In our proposed method, we find that it is easy to increase the tracking speed, to reduce the design complexity, and to obtain the accurate value of code delay and Doppler frequency.

1.2 Motivation and Literatures Review

Although GPS signal tracking is a mature subject, there is still some ways to improve the tracking speed and the design complexity. A Costas loop tracking method is presented in [2] and [1]; it is using the early-late method to find the code delay and Doppler frequency via a PI loop filter. Another loop filter in the DPLL is presented in [13]; it is using a fuzzy bandwidth controller (FBC) to realize the loop filter, and the FBC provides a time-varying bandwidth. Due to the structure of the DDLL and DPLL system, we can design different kind of loop filters. In the methods discussed above, the filter design is uncertain as a result of more fluctuant performance if we design the filter inadequately. In reference [15], a new method is that a extended Kalman filter is used to obtain the code delay in the presence of the multipath. In reference [14], they propose a space-time adaptive processing (STAP) algorithm for delay tracking and acquisition of the GPS signature sequence using the extended Kalman filter (EKF), and the algorithm is shown to track the desired timing having high speed and fine resolution. The DDLL and DPLL model are presented in [3]. In our proposed method, we apply the idea of [14] and [15] to establish the state-space model of the EKF based on the structure of the DDLL and DPLL model [3]. It can obtain the fine resolution without increasing design complexity.

1.3 Organization of the Thesis

The remainder of this thesis is divided into four chapters including conclusions. Chapter 2 reviews the GPS receiver, the GPS signal, and the acquisition method. Chapter 3 illustrates the difference between the current method and our method. Chapter 4 demonstrates the computer simulations. The final chapter is the conclusions.

Chapter 2

GPS SIGNAL MODEL

2.1 Introduction to GPS

GPS is a spaced-based, worldwide, all-weather, navigation and timing system which is designed to provide precise position, velocity, and timing information on a global common coordinate system to an unlimited number of suitably equipped users.Now, GPS becomes the most important navigation system. It consists of three segments: the space-segment, the control-segment, the user-segment. When full deployed, the space-segment will contain 24 satellites divided into six orbits and each orbit has four satellites. Each orbit makes a 55-degree angle with the equator, which is referred to as the inclination angle. The orbit are separated by 60 degree to cover the complete 360 degree, and the satellite constellation provides a 24-hr global user navigation. The radius of the satellite orbit is 26,560 km and the nominal orbital period of a GPS satellite is one-half of a sidereal day or 11 hr 58 min. Table 2.1 lists all the parameter.

The control-segment consists of monitor stations to check the health of the satellites, to determine their orbits (called station keeping). The control-segment also monitors the satellites solar array, battery power levels, and propellant levels used for maneuvers and activates spare satellites. The control-segment update the each satellite's clock, ephemeris, and almanac data in the navigation message once per day or as needed. To accomplish the above functions, the control-segment includes three different physical components: the master control station, monitor stations, and the ground uplink antennas. The

Constellation	
Number of satellites	24
Number of orbital planes	6
Number of satellites per orbit	4
Orbital inclination	55^o
Orbital radius	26560 km
Period	11 hrs 57 min 57.26 sec
Ground track repeat	sidereal day

Table 2.1: Characteristics of GPS Satellites

master control station process data from the monitor stations for correcting the satellite clock, and updating ephemeris and almanac data for each satellite. The monitor stations collect the satellite signal, and transmit it to the master control station. The ground uplink antenna facility provides the means of commanding and controlling the satellites and uploading the navigation data and other data. The user-segment, typically referred to as a "GPS receiver," processes the signal transmitted from the satellite to determine the user position. The initial GPS receiver manufactured in the mid-1970s was heavy, large, and bulky. With today's technology, a GPS receiver weighting a few pounds and occupying a small volume is more capability.

In order to determine the absolute position, a user need to receive signals from four different GPS satellites. Two satellites and two distances give two possible solutions because two circles intersect at two points. A third circle is need to uniquely determine the user position. In the above discussion, the distance measured from the user to the satellite is assumed very accurate and there is no bias error. In fact, the constant unknown bias error exists between the satellite and the user, because the user clock is usually different from the satellite clock. Therefore, in order to find the accurate user position, four different GPS satellites are needed.

A GPS satellite transmit information to the user on two different L-band frequencies L1 and L2. The center frequency of L1 is at 1575.42 MHz and L2 is at 1227.6 MHz. All frequencies in the space vehicle are integral multiples of the 10.23 MHz clock. The

frequencies are very accurate, because their reference is an atomic clock.

The GPS signal is modulated with two PRN codes: the Precision (P) code which provides for precise measurement and the Coarse/Acquisition (C/A) code which provides for coarse measurement. The actual P code is not directly transmitted by the satellite, but it is modulated by A Y code, which is often referred to as the P(Y) code. At the present time, the L1 frequency contains the P(Y) code and the C/A code, and the L2 frequency contains only the P(Y) code. Both the L1 and L2 signals are modulated with the navigation data bit stream at 50 bps. We will consider the C/A code only in our discussion below.

2.1.1 GPS Receiver

The GPS receiver consists of several elements: antenna, preamplifier, theta ,prefilter, reference oscillator, frequency synthesizer, RF/IF downconverter, A/D converter and digital signal processing (DSP). A GPS antenna should cover a wide spatial angle to receive the maximum number of signals. The antenna should reject multipath effect and interference. A jamming or interference signal usually comes from a low elevation angle. Sometimes an antenna will have a higher elevation angle to avoid signals from a low elevation angle. Therefore, the trade-off between the maximum number of signals and the interference signal to achieve the best performance. The most important argument in the antenna is the gain, and the antenna should have uniform gain over a wide spatial angle. Because of the right-handed circularly polarized GPS signal, the antenna is the same right-handed circularly polarized to have a higher gain.

The preamplifier generally consists of two elements: filter and low noise amplifier (LNA). The filter in front of or behind the LNA removes the undesired signal out. For the C/A code receiver in the L1 band, the bandwidth of the filter is 2 MHz at least, because the C/A code bandwidth is 2.046 MHz. The LNA amplifies the received signal and improves the noise response. The LNA gain is normally from 25 to 40 dB. The noise figure of the LNA is from 3 to 4 dB because of the insertion loss.

The reference oscillator provides the standard of time and frequency for the receiver. Because the GPS navigation bases on the transmitting time, the reference oscillator is the important element in the GPS receiver. The reference oscillator output is synthesized by

the frequency synthesizer to generate the frequency for the acquisition and tracking loop. The synthesizer generates the signal frequency for receiving and processing received signal. Every GPS receiver must have the frequency planning such as the intermedia frequency (IF) range and the sampling frequency. The synthesizer output mainly generates the local oscillator and the sampling frequency, etc, to conform with the frequency planning. The synthesizer employs the numerically controlled oscillator (NCO) to generate the desired frequency.

The RF/IF downconverter down converts the RF signal to the intermediate signal. The higher frequency component of the downconverter output would be filtered out. Although the frequency of the filter output is in the designed bandwidth, the strength is differential due to the environment or the receiving position. The signal strength adjusted by the automatic gain control (AGC) circuit is useful to process the received signal. The down converted signal will be digitized by an ADC. The digitized signal is transmitted into the DSP circuit. The DSP circuit will estimate the doppler frequency and the time delay for the navigation through the acquisition and tracking loop.Thus, we can demodulate the C/A code and the satellite positions can be obtained.

Assume that there are three known locations at (x_1, y_1, z_1), (x_2, y_2, z_2), and (x_3, y_3, z_3), and an unknown location (x_u, y_u, z_u) in Figure 2.1. The measured distances between the known locations and the unknown location can be written as

$$\begin{aligned} \rho_1 &= \sqrt{(x_1 - x_u)^2 + (y_1 - y_u)^2 + (z_1 - z_u)^2} \\ \rho_2 &= \sqrt{(x_2 - x_u)^2 + (y_2 - y_u)^2 + (z_2 - z_u)^2} \\ \rho_3 &= \sqrt{(x_1 - x_u)^2 + (y_1 - y_u)^2 + (z_1 - z_u)^2} \end{aligned} \tag{2.1}$$

Because there are three unknown arguments and three equations, x_u, y_u, and z_u can be determined from the three equations. The nonlinear equation cannot be solved directly, but can be solved with linearization and an iterative method.

Every satellite sends a signal at a certain time t_{si}. The receiver will receive the signal at a later time t_u. The distance between the user and the satellite i is

$$\rho_{iT} = c(t_u - t_{si}) \tag{2.2}$$

where c is the speed of light, ρ_{it} is referred to as the true pseudorange from the user to

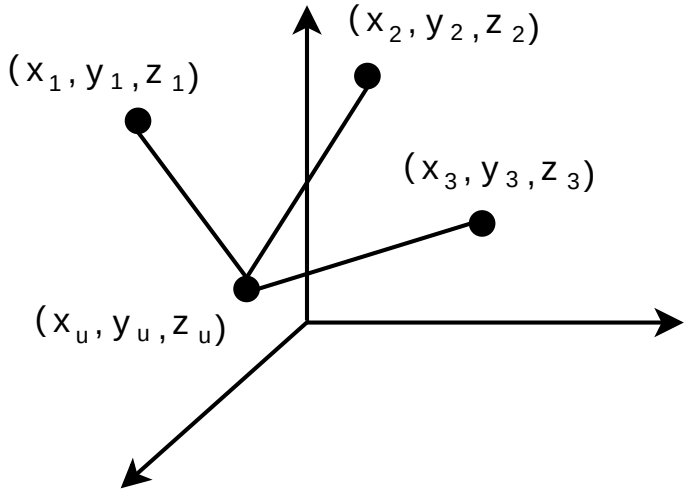

Figure 2.1: Use the three known positions to find one unknown position

the satellite i, t_{si} is referred to as the true transmission time, t_u is referred to as the true reception time.

It is impossible to obtain the correct time from the satellite to the user. The actual satellite clock time t'_{si} and actual user clock time t'_u are related to the true time as

$$\begin{aligned} t'_{si} &= t_{si} + \Delta b_i \\ t'_u &= t_u + b_{ut} \end{aligned} \tag{2.3}$$

where Δb_i is the satellite clock error, b_{ut} is the user clock bias error. The user clock error cannot be corrected through received information. As a result, Equation 2.1 must be modified as

$$\begin{aligned} \rho_1 &= \sqrt{(x_1 - x_u)^2 + (y_1 - y_u)^2 + (z_1 - z_u)^2} + cb_{ut} \\ \rho_2 &= \sqrt{(x_2 - x_u)^2 + (y_2 - y_u)^2 + (z_2 - z_u)^2} + cb_{ut} \\ \rho_3 &= \sqrt{(x_1 - x_u)^2 + (y_1 - y_u)^2 + (z_1 - z_u)^2} + cb_{ut} \end{aligned} \tag{2.4}$$

The navigation computer computes the user position by the pseudorange. In order to find the pseudorange, we must determine the transmission time from the satellite to the user by the C/A data acquisition and tracking. Therefore, in this thesis we focus on the tracking of C/A code.

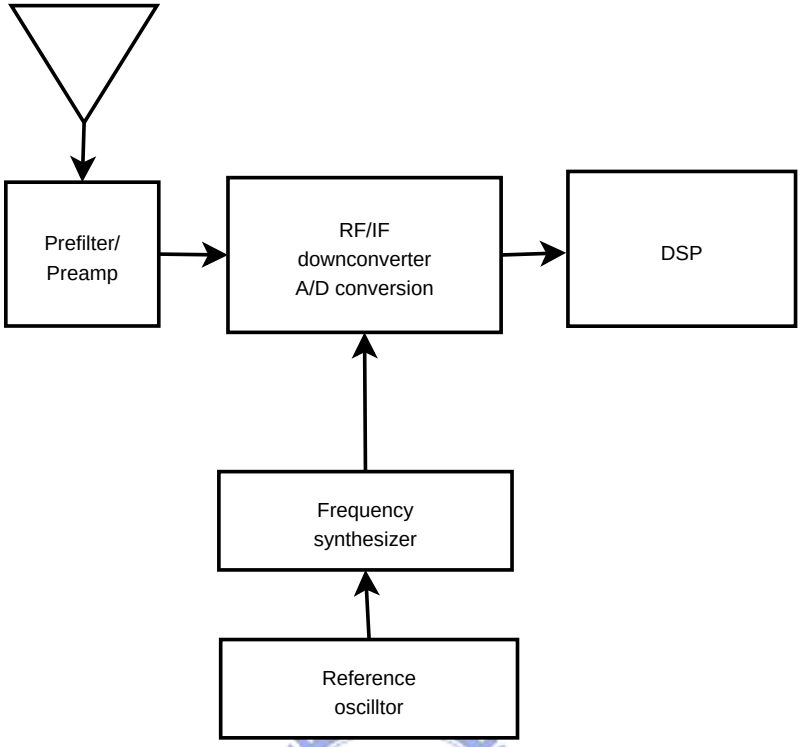

Figure 2.2: The block diagram of GPS receiver and DSP

2.1.2 RF Module

The RF frequency downconverter consists of a mixer and a band-pass filter as shown in Fig 2.3.The RF module converts the RF signal frequency down to the intermedia frequency (IF). The reference clock frequency is 24.5535 MHz.The local oscillator generates the NCO signal whose frequency is 1571.424 (24.5535×64=1571.24) MHz. The mixer output signal frequency referred to as the IF is 3.996 (1575.42-1571.424=3.996) MHz. Thus, the bandwidth of the bandpass (BP) filter is 6 MHz. The A/D converter samples the

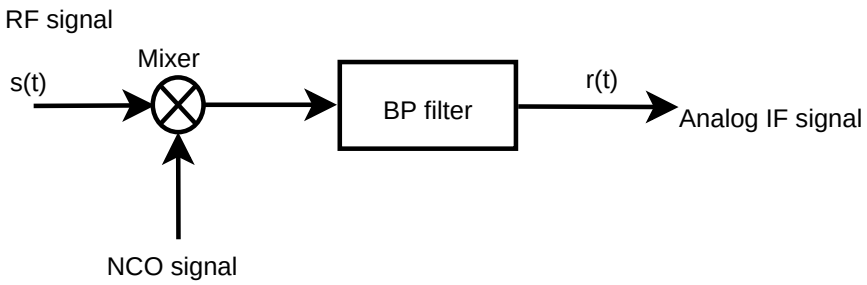

Figure 2.3: RF Module

IF signal and outputs the discrete IF signal to the DSP.

2.1.3 A/D Converters

According to the Nyquist sampling theorem [ref], the sampling frequency f_s must be twice the maximum frequency f present in the input signal to avoid aliasing error.Therefore, the sampling rate for the C/A code signal should be

$$f_s \geq 2 \times 1.023\text{MHz} = 2.046\text{MHz} \tag{2.5}$$

Because of the practical ic specification, we select the sampling frequency f_s=6.138375 MHz.

2.2 GPS Signal from The Satellite

2.2.1 Signal Structure

The GPS signal contains two frequency components: link 1 (L1) and link 2 (L2). The centre frequency of L1 is at 1575.42 MHz and L2 is at 1227.6 MHz. These frequencies are coherent with multiple of a fundamental clock rate f_0=10.23 MHz such that

$$\begin{aligned} L1 &= 1575.42\text{MHz} = 154 \times 10.23\text{MHz} \\ L2 &= 122.76\text{MHz} = 120 \times 10.23\text{MHz} \end{aligned} \tag{2.6}$$

These frequencies are very accurate because their reference is an atomic frequency standard. But when the GPS receiver receives the signals, they are not at the desired frequency. The relative motions between the satellite and receiver produce the doppler frequency effect which is approximately $\pm$5 KHz.

The L1 signal consists of both in-phase and quadrature signals, and we only consider the quadrature part. The quadrature part is modulated by the C/A signal, and it can be written as:

$$S_i(t) = AP(t)D(t)\sin(2\pi ft + \phi) \tag{2.7}$$

where S_i is the signal transmitted by satellite i, A is the amplitude of the C/A code, ϕ is the initial phase, $P(t) = \pm 1$ represents the phase of the C/A code, f is the L1 frequency, and $D(t) = \pm 1$ represents the data code.

2.2.2 Generation of C/A Code

The GPS C/A code is a kind of Pseudorandom noise (PRN) codes known as the Gold code [reference communication] with a noiselike waveform that is generated by the feedback shift register, its initial state, and the feedback logic. If the feedback shift register has n bits, the sequence length is $2^n - 1$. The GPS C/A code signal is generated by the product of two PRN sequence G1 and G2. The two 10-bit feedback shift registers generate the periodic PRN sequence G1 and G2 whose length are both $2^{10} - 1 = 1023$ bits. The feedback circuit of the feedback register is accomplished with the modulo-2 adder (exclusive or).

The different stage of the shift register fed to the modulo-2 adder determines the different PRN sequence. It is common to describe the design of the feedback circuit by the polynomial form $1 + \sum x^i$, where x^i means that the output of the ith cell of the shift register is used to as the modulo-2 adder input. The polynomial form of the G1 and G2 generator are:

- G1 : $1 + x^3 + x^{10}$
- G2 : $1 + x^2 + x^3 + x^6 + x^8 + x^9 + x^{10}$

as shown in Figure 2.4. The last bit of the shift register is referred to as the maximum-length sequence (MLS) output. The another modulo-2 adder combines the G1 generator MLS output and the G2 generator delayed output to generate the C/A code. This allows the generation of 36 unique C/A code phases using the same structure code generator. The delayed output of the G2 generator is equivalent to the exclusive-or of selected two bits of the shift register. The initial value of the G1 and G2 generator are all 1's.

Table lists the code phase assignment. For example, the G2 generator selects the second and tenth bit of the shift register to generate the C/A code of the satellite 6. With

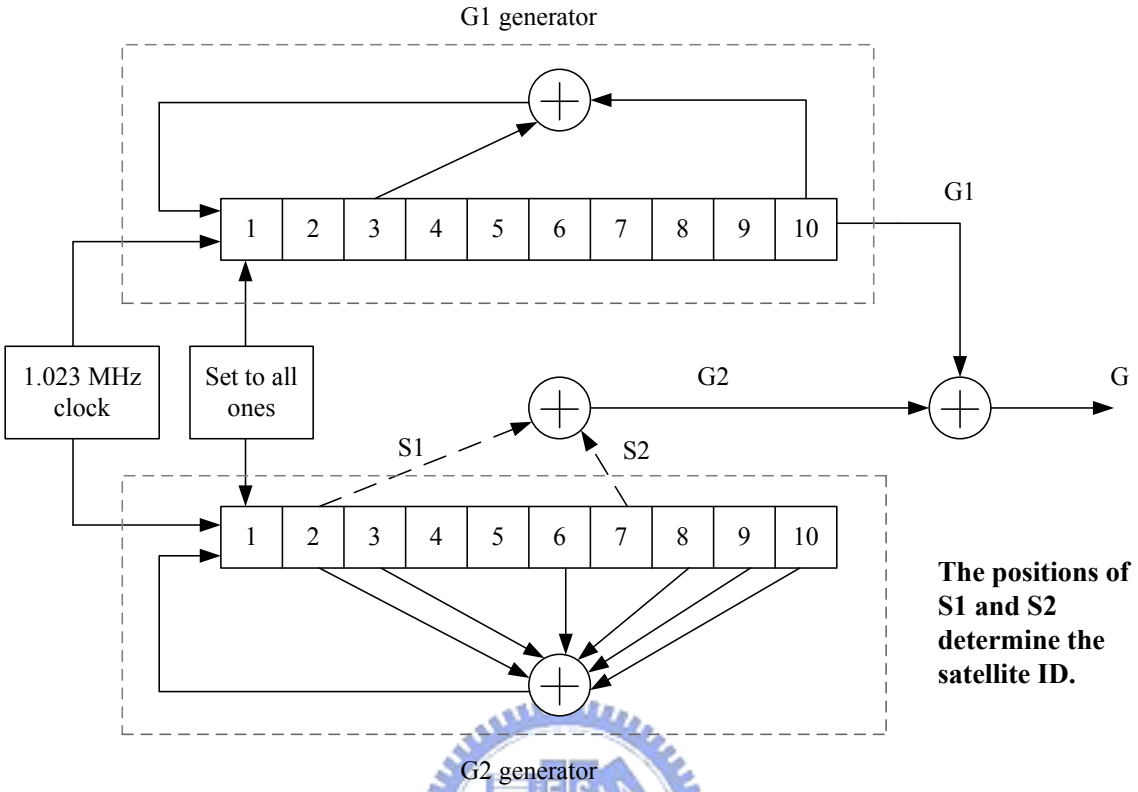

Figure 2.4: C/A code generator

this selection, the G2 output equals the MLS ouput delayed 18 bits. The last column of Table is 1455, which means 101010 in binary form. If the first 10 generated C/A code do not match the binary form, the code is incorrect.

The important property of the C/A code is the autocorrelation characteristics. The maximum autocorrelation peak is 1023 being equal to the C/A code length as shown in Figure .The autocorrelation peak of the weak signal must be higher than the cross-correlation peaks from the strong signals in order to detect the weak signal. The Gold codes are near orthogonal, and the cross correlations have small values. The cross-correlation values are: -65/1023 (occurrence 12.5%), -1/1023 (occurrence 75%), and 63/1023 (occurrence 12.5%) as shown in Figure 2.5.

2.2.3 Data Format

The navigation data stream modulated with the C/A code is at 50 bit per second. Thus, the consecutive 20 C/A codes have the same data bit. Thirty data bits compose a navi-

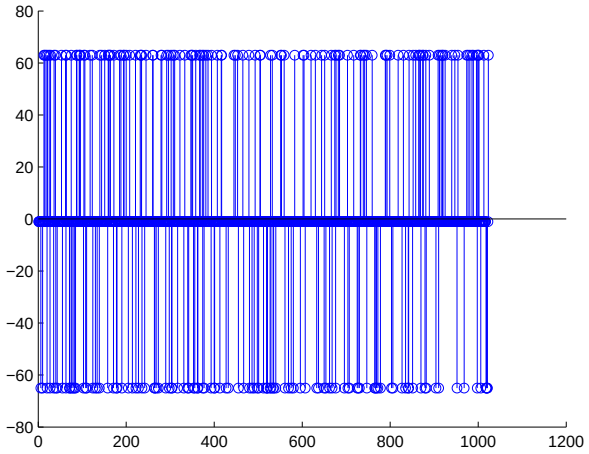

Figure 2.5: Cross-correlation of satellite 19 and 31

gation word that is 600 ms long. Ten words compose a subframe that is 6 seconds long. Five subframes compose a page that is 30 seconds long. Twenty-five pages compose a complete data set that is 12.5 minutes long. If we can receive the first three of a page from four satellites, the user position can be determined. Figure 2.6 shows the GPS data format.

2.3 Signal Model of The Digital Baseband Processor

Considering a single channel in the digital baseband processor , the input discrete signal plus noise from the A/D converter can be modeled as:

$$r(n) = AP[(1+\zeta)nT_s - \xi T_p]D(n)e^{j((\omega_b+\omega_d)n+\phi_0)} + v(n) \tag{2.8}$$

where P[·] is a ± 1 - valued C/A code with rate R(P), $D(n)$ is the data bit, delayed by τ = ξT_p with respect to GPS system time, ω_b = 2 $\pi f_b T_s$ and ω_d = 2 $\pi f_d T_s$ are digital radian frequencies corresponding to the intermedia carrier frequency f_b and doppler shift f_d, ϕ_0 is the initial phase phase at n = 0, T_s is the sampling period, T_p is the code chip width, and $v(n)$ is a Gaussian white noise. The code rate R(P) is equal to (1+ζ) R_0(P) because of the doppler effect, where ζ = f_d / f_L, and R_0(P) is the code rate without doppler effect.

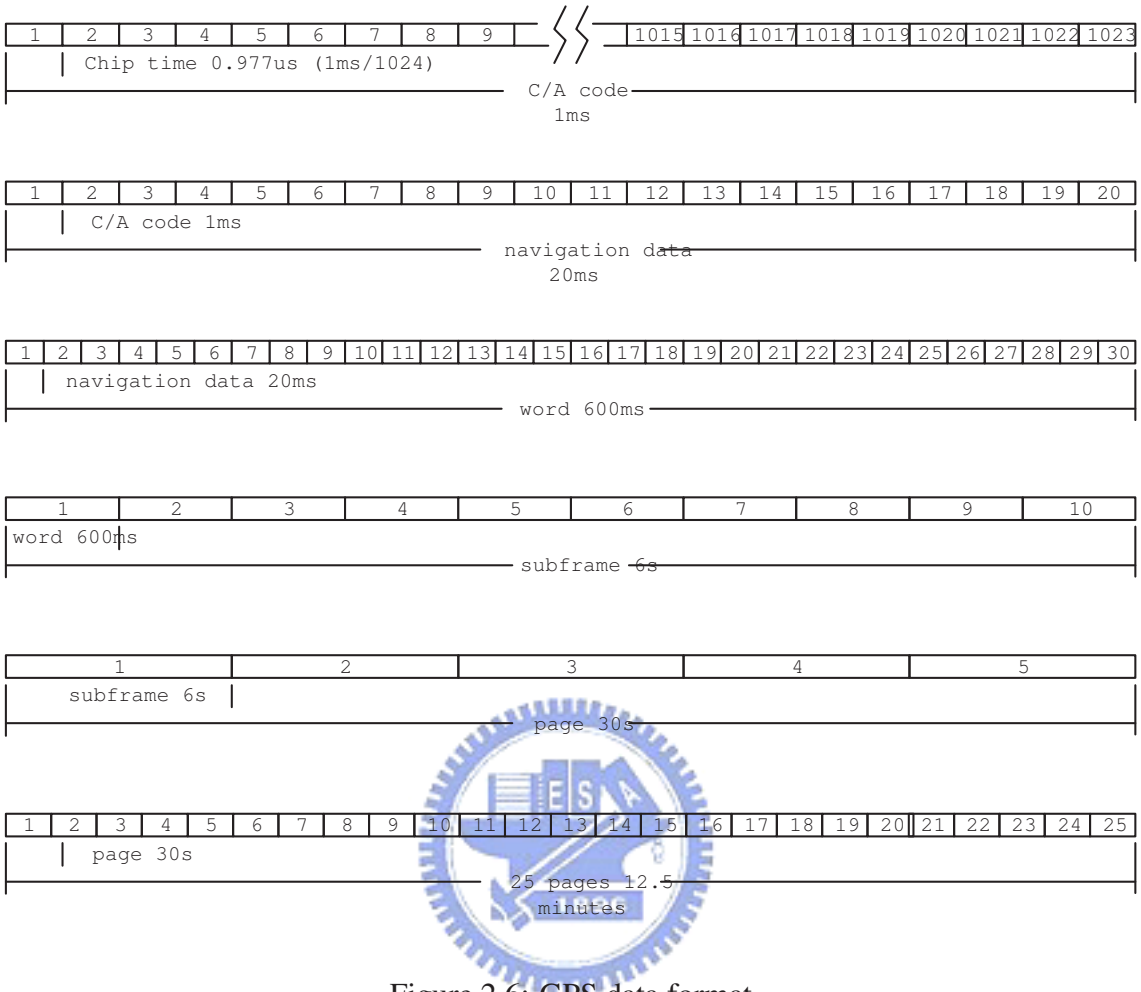

Figure 2.6: GPS data format

2.4 C/A Code Acquisition

The pseudorange between the satellite and the receiver is measured by means of synchronizing the input PRN code phase with the locally generated PRN code phase, which is accomplished by the two steps: acquisition and tracking. In order to track and decode the information in the GPS signal, an acquisition method must be used to detect the Doppler frequency and the coarse code phase of the input signal first. The uncertainty range of the Doppler frequency of the L1 signal is from -5 kHz to 5 kHz for a static receiver. The begging of the C/A code and the Doppler frequency are the parameters passed to the tracking loop. Three acquisition methods will be mentioned: the conventional, the Fast Fourier Transform (FFT), and the Chirp Transform Algorithm (CTA).

The conventional method employs the correlation operation to find the coarse code

phase delay and the coarse Doppler frequency [1][1]. The FFT method can be considered as a reduced computational version of the conventional method [2]. The CTA method can obtain better frequency resolution and less computation complexity than the FFT method [12].

Chapter 3

C/A CODE TRACKING

In the previous chapter, C/A code acquisition provides us the coarse code delay and Doppler frequency shift. In order to obtain the precise code delay and accurate Doppler frequency shift, the tracking loop is needed. The time delay resolution is within about one-half chip time, and the frequency resolution is within about hundreds of Hertz from the acquisition loop. The pseudorange due to the estimated time delay of the acquisition loop is 146 m (977.5 ns $\times$ 3 $\times$ 10^8 m/s). The pseudorange resolution is too bad to be used to position the user. Thus, the pseudorange due to the time delay resolution in the tracking loop is within about 10-30 m. The range of the time delay that can be handled by the tracking loop is one-half chip time, and the range of the Doppler frequency loop is hundreds of Hertz, too. In order to track the code delay and the Doppler frequency, digital delayed-locked loop (DDLL) and digital phase-locked loop (DPLL) are needed.

3.1 DDLL Model

Accurate code delay synchronization between the input and local PRN code signal is accomplished by a simplified block diagram of the DDLL as shown in Figure 3.1. The code phase discriminator detects the phase error between the input signal and the local PRN code signal. A practical implementation of the code phase discriminator is the early-late correlation operation between the input signal and the local PRN codes. The Figure 3.2 shows the fundamental block diagram of the early-late operation. The PRN code

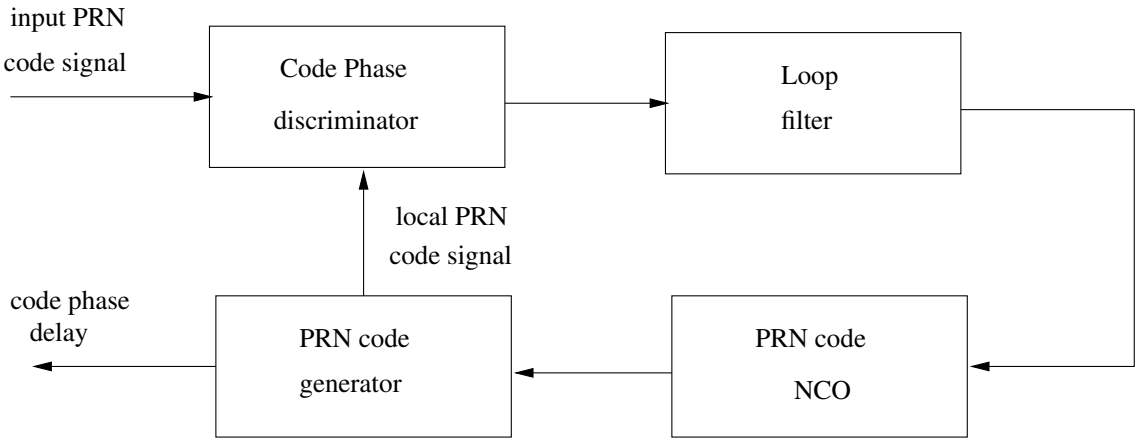

Figure 3.1: Simplified Block Diagram of the DDLL

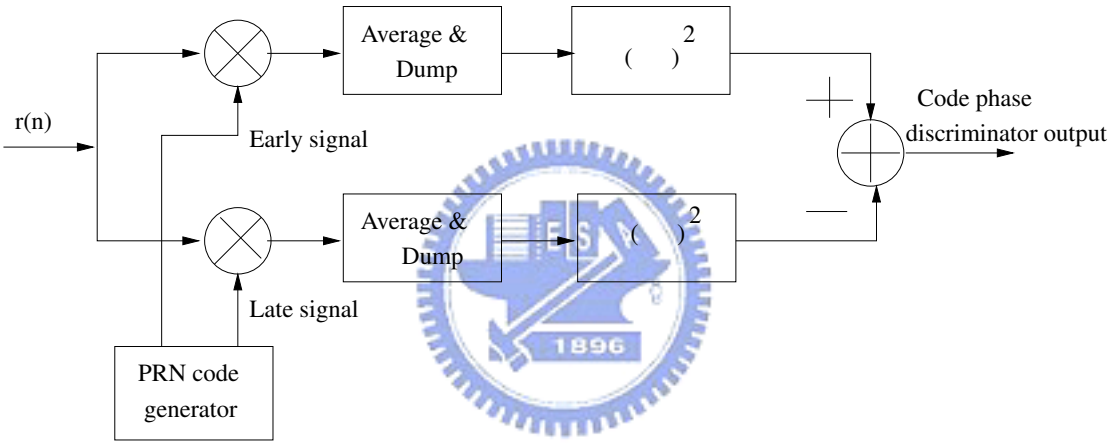

Figure 3.2: Simplified Block Diagram of the Early-Late Operation

generator generates the early, prompt, and late code which are approximately one-half-chip time (0.498 us) apart or less. The prompt code is used to strip the PRN code from the input signal. The early and late code correlate with the input PRN code to produce two outputs. Each output passes through a "Average & Dump" filter, and the filter output is squared. The two squared outputs are compared with each other to generate a control signal. According to the PRN code theory [5], if the prompt PRN code is aligned with the input PRN code, the early and late channel outputs y_e and y_l are equal, and the error signal which is generated by the code phase discriminator is zero as shown in Figure 3.3, where δ is the relative code phase offset of the early and late correlators, and y_p is that the prompt code correlates the input PRN code. The error signal from the code phase discriminator

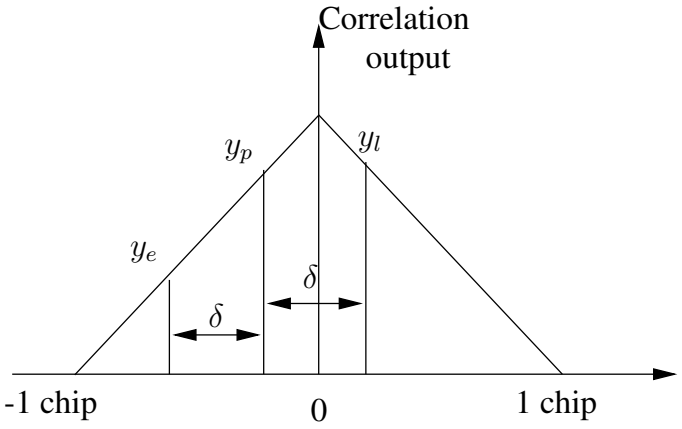

Figure 3.3: Correlation output of a PRN code

passes to the loop filter. The loop filter output is to control the PRN code generator as shown 3.1. In the conventional method, the loop filter is a PI filter. In this thesis, our proposed method is that the Kalman filter will replace the PI filter. The code delay tracking loop to be modelled here is a noncoherent, early-late, digital delay-locked loop, with two independent correlators for discriminating code phase error, as shown in Figure 3.4. The function of the DDLL is to track the time delay of the input digital spreading PRN code signal $P[(1+\zeta)nT_s - \xi T_p]$. The parameter $\hat{\xi}(t)T_p$ represents the receiver estimate of $\xi(t)T_p$, and $\rho(t) = \xi(t) - \hat{\xi}(t)$ is the time delay tracking error normalized by a PRN code chip time.

As mentioned in (2.8), the input discrete signal model is

$$r(n) = AP[(1+\zeta)nT_s - \xi T_p]D(n)e^{j((\omega_b+\omega_d)n+\phi_0)} + v(n) \tag{3.1}$$

With "+" sign representing the early (E) correlator and "-" sign representing the late (L) correlator, the local early and late signals are

$$I_{I+}(n) = AP[(1+\hat{\zeta})nT_s - \hat{\xi}T_p + \delta T_p]e^{-j((\omega_b+\hat{\omega}_d)n)} \tag{3.2}$$

$$I_{I-}(n) = AP[(1+\hat{\zeta})nT_s - \hat{\xi}T_p - \delta T_p]e^{-j((\omega_b+\hat{\omega}_d)n)} \tag{3.3}$$

where δ represents the relative code phase offset of the early and late correlators. The

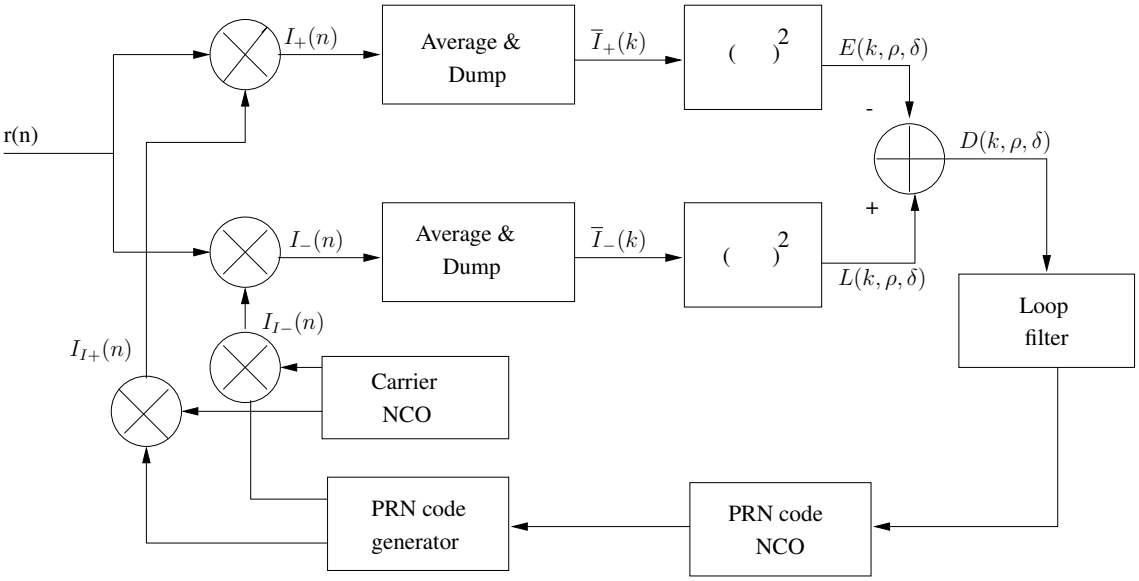

Figure 3.4: Block Diagram of Early-Late DDLL

outputs of the mixer which mix the input discrete signal with the local signal are

$$I_+(n) = r(n)I_{I+}(n) \tag{3.4}$$

$$I_-(n) = r(n)I_{I-}(n) \tag{3.5}$$

The outputs of the mixer are through the "Average & Dump" LP filter, and the components of frequency $(2\omega_b + \omega_d + \hat{\omega_d})$ in both early and late channel will be suppressed.The LP filter output of the k-th correlation interval are

$$\overline{I}_+(k) = \frac{1}{N}\sum_{n=0}^{N-1} AP[(1+\zeta)nT_s - \xi T_p]P[(1+\hat{\zeta})nT_s - \hat{\xi}T_p + \delta T_p] \times D(n)e^{j(\Delta\omega_d(k)n+\phi_{k-1})} + v_{I+}(k) \tag{3.6}$$

$$\overline{I}_-(k) = \frac{1}{N}\sum_{n=0}^{N-1} AP[(1+\zeta)nT_s - \xi T_p]P[(1+\hat{\zeta})nT_s - \hat{\xi}T_p - \delta T_p] \times D(n)e^{j(\Delta\omega_d(k)n+\phi_{k-1})} + v_{I-}(k) \tag{3.7}$$

where $\Delta\omega_d(k) = \omega_d(k) - \hat{\omega_d}(k)$ is the error of the Doppler frequency shift in the k-th

correlation interval.The noise components through the LP filter are

$$v_{I+}(k) = \frac{1}{N}\sum_{n=0}^{N-1} v(n)P[(1+\hat{\zeta})nT_s + \hat{\xi}T_p + \delta T_p] \times e^{j((\omega_b(k)+\hat{\omega}_d(k))n+\hat{\phi}_{k-1})} \tag{3.8}$$

$$v_{I-}(k) = \frac{1}{N}\sum_{n=0}^{N-1} v(n)P[(1+\hat{\zeta})nT_s - \hat{\xi}T_p - \delta T_p] \times e^{j((\omega_b(k)+\hat{\omega}_d(k))n+\hat{\phi}_{k-1})} \tag{3.9}$$

When $|\Delta\omega_d(k)N| \ll 1$, (3.7) can be approximated to [3]

$$\begin{aligned}
\overline{I}_+(k) &= \frac{1}{N}\sum_{n=0}^{N-1} AP[(1+\zeta)nT_s - \xi T_p]P[(1+\hat{\zeta})nT_s + \hat{\xi}T_p + \delta T_p] \\
&\quad \times D(n)sinc[\Delta\omega_d(k)N/2]e^{j(\Delta\omega_d(k)N/2+\phi_{k-1})} + v_{I+}(k) \\
\overline{I}_-(k) &= \frac{1}{N}\sum_{n=0}^{N-1} AP[(1+\zeta)nT_s - \hat{\xi}T_p]P[(1+\hat{\zeta})nT_s - \hat{\xi}T_p - \delta T_p] \\
&\quad \times D(n)sinc[\Delta\omega_d(k)N/2]e^{j(\Delta\omega_d(k)N/2+\phi_{k-1})} + v_{I-}(k)
\end{aligned} \tag{3.10}$$

The PRN code autocorrelation term is expressed as

$$\frac{1}{N}\sum_{n=0}^{N-1} P[(1+\zeta)nT_s - \xi T_p]P[(1+\hat{\zeta})nT_s + \hat{\xi}T_p \pm \delta T_p] \triangleq R(\rho \pm \delta) \tag{3.11}$$

where $R(\rho \pm \delta) \triangleq E[P[(1+\zeta)nT_s - \xi T_p]P[(1+\hat{\zeta})nT_s + \hat{\xi}T_p + \delta T_p]]$ is the autocorrelation function of PRN code, $\rho = \xi - \hat{\xi}$ is the normalized delay error, $\hat{\zeta} = \hat{f}_d/f_L$, δ is the normalized local PRN code phase offset. Therefore (3.10) is simplified as

$$\overline{I}_+(k) = AR(\rho(k)+\delta) \times D(n)sinc[\Delta\omega_d(k)N/2]e^{j(\Delta\omega_d(k)N/2+\phi_{k-1})} + v_{I+}(k) \tag{3.12}$$

$$\overline{I}_-(k) = AR(\rho(k)-\delta) \times D(n)sinc[\Delta\omega_d(k)N/2]e^{j(\Delta\omega_d(k)N/2+\phi_{k-1})} + v_{I-}(k) \tag{3.13}$$

The outputs of the early and late correlators are

$$E(k,\rho,\delta) = \overline{I}_+^2(k) \tag{3.14}$$

$$L(k,\rho,\delta) = \overline{I}_-^2(k) \tag{3.15}$$

The output of the code phase discriminator is then

$$D(k,\rho,\delta) = L(k,\rho,\delta) - E(k,\rho,\delta) \triangleq K_0 D_\Delta(k,\rho,\delta) + v_D(k,\rho,\delta) \tag{3.16}$$

where

$$K_0 = A^2 D^2(n) sinc^2[\Delta\omega_d(k)N/2] \tag{3.17}$$

$$D_\Delta(k,\rho,\delta) = R^2(\rho(k)-\delta) - R^2(\rho(k)+\delta) \tag{3.18}$$

The discriminator $D_\Delta(k,\rho,\delta)$ S-curves for the noncoherent early-late DDLL is plotted in Figure 3.5. and $v_D(k,\rho,\delta) = n_1(k) + n_2(k)$ with

$$n_1(k) = v_{I-}^2(k) - v_{I+}^2(k) \tag{3.19}$$

$$n_2(k) = [v_{I-}(k) - v_{I+}(k)] \times [2AD(n)sinc[\Delta\omega_d(k)N/2]e^{j(\Delta\omega_d(k)N/2+\phi_{k-1})}] \tag{3.20}$$

The autocorrelation of $v_D(k,\rho,\delta)$ is [3]

$$R_{v_D}(i) = 2(\frac{N_0 B_L}{2})^2[1-R^2(2\delta)] + A^2D^2(n)[\frac{1}{2}(\frac{N_0 B_L}{2})] \times sinc^2[\Delta\omega_d N/2] f(\rho(k),\delta)\delta(i) \tag{3.21}$$

where $B_L = \pi/N(rad)$, $f(\rho(k),\delta) = R^2(\rho(k)-\delta)+R^2(\rho(k)+\delta)-2R(\rho(k)-\delta)R(\rho(k)+\delta)R(2\delta)$, and N_0 is the power spectral density of $v(n)$,

3.2 DPLL Model

A digital phase-locked loop is used to extract the accurate carrier phase of the input GPS signal by differencing the incoming Doppler-shifted carrier with locally generated signal. The DPLL consists of a loop filter, a carrier phase discriminator, and a numerically controlled oscillator (NCO) as shown in Figure 3.6. The phase discriminator works on the output of the "Average & Dump" filter to detect the phase error between the input signal and the locally generated signal. The phase discriminator is an arctangent comparator commonly. The phase discriminator output passes through the loop filter to generate the control signal. The PI filter is selected as the loop filter in generally. The control signal is used to tune the NCO to generate a carrier frequency to follow the input frequency. The NCO output may be used to remove the carrier frequency component of the input signal, and at the same time, the phase and Doppler frequency may be obtained from the phase and frequency of the NCO. The NCO generates the local reference signal at sampling rate

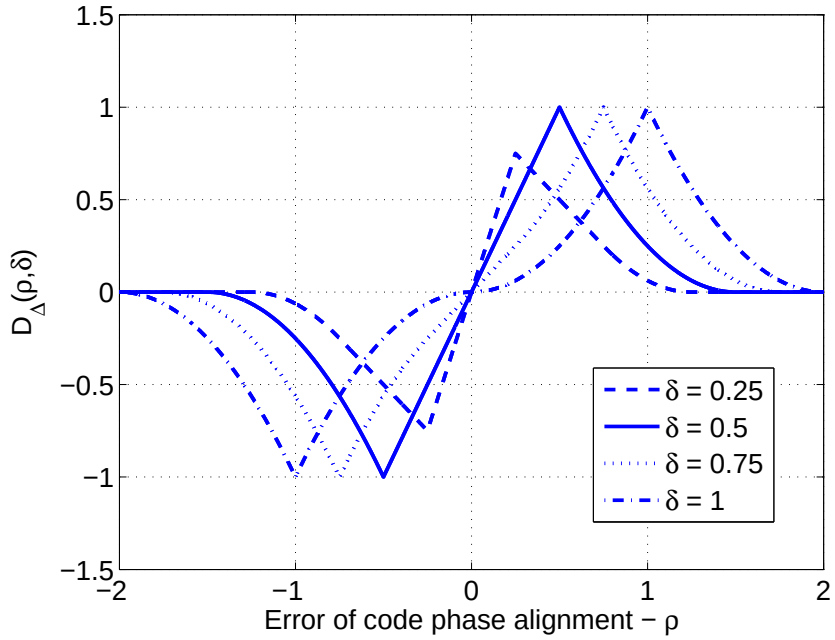

Figure 3.5: Discriminator S-Curve of Noncoherent Early-Late DDLL

f_s, and the output of the loop filter modifies the phase and frequency of the NCO every NT_s. The DPLL model can be shown in Figure 3.7.

The signal input to the DBP defined in (2.8) is rewritten as

$$r(n) = AP[(1+\zeta)nT_s - \xi T_p]D(n)e^{j((\omega_b+\omega_d)n+\phi_0)} + v(n) \tag{3.22}$$

Combining the local PRN code signal and NCO signal, the local signal $Q_Q(n)$ is

$$Q_Q(n) = P[(1+\hat{\zeta})nT_s + \hat{\xi}T_p]e^{-j((\omega_b+\hat{\omega}_d)n)} \tag{3.23}$$

With the input $r(n)$ and $Q_Q(n)$, the correlation output of the mixer is

$$Q(n) = r(n)Q_Q(n) \tag{3.24}$$

In the k-th correlation interval, the output of the "Average & Dump" filter is

$$\overline{Q}(k) = \frac{1}{N}\sum_{n=0}^{N-1} AP[(1+\zeta)nT_s - \xi T_p]P[(1+\hat{\zeta})nT_s - \hat{\xi}T_p + \delta T_p] \times D(n)e^{j(\Delta\omega_d(k)n+\phi_{k-1}-\hat{\phi}_{k-1})} + v_Q(k) \tag{3.25}$$

where $\Delta\omega_d(k) = \omega_d(k) - \hat{\omega}_d(k)$, $\phi(k-1)$ is the accumulated phase component generated by the previous input signal, and the general form is expressed as

$$\phi(k) = (\omega_b + \omega_d(k)) \times N + \phi(k-1) \tag{3.26}$$

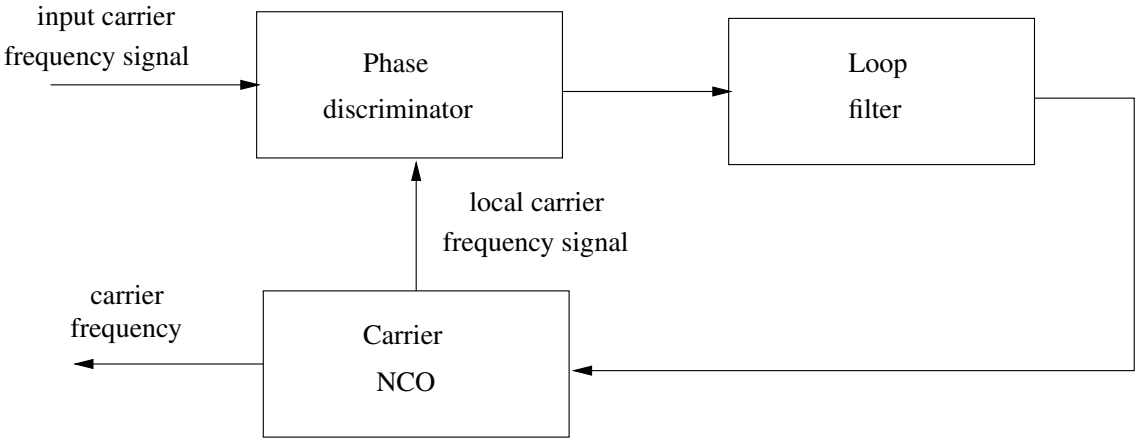

Figure 3.6: Simplified Block Diagram of the DPLL

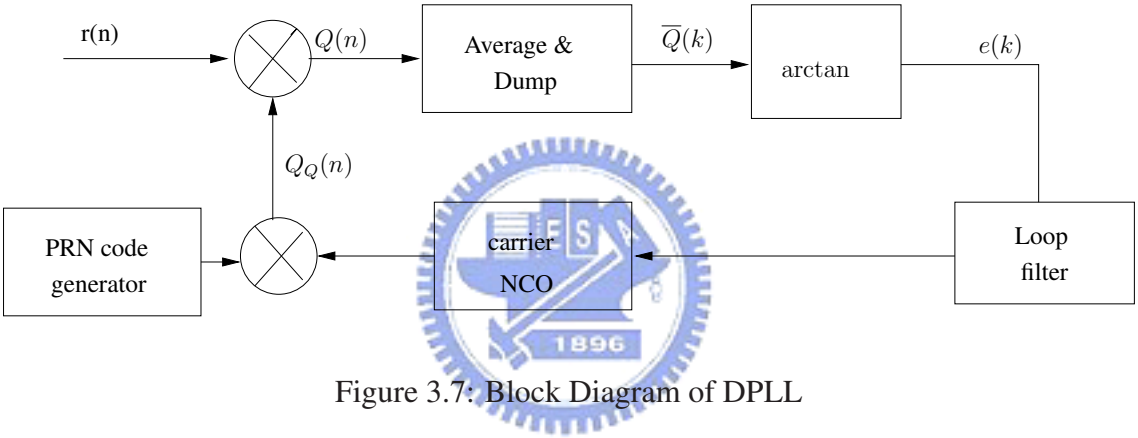

Figure 3.7: Block Diagram of DPLL

$\phi(k-1)$ is the accumulated phase component generated by the previous local signal, and the general form is expressed as

$$\hat{\phi}(k) = (\omega_b + \hat{\omega}_d(k)) \times N + \hat{\phi}(k-1) \tag{3.27}$$

We follow the procedure similar to that of deriving (3.13), and the approximated equation is written as

$$\overline{Q}(k) = AR(\tau - \hat{\tau})D(n)sinc[\Delta\omega_d(k)N/2]e^{j(\Delta\omega_d(k)+\phi(k-1)-\hat{\phi}(k-1))} + v_Q(k) \tag{3.28}$$

where $\tau = \xi T_p$ and $\hat{\tau} = \hat{\xi} T_p$.

The phase discriminator performs the arctangent operation, which has the output

$$\begin{aligned} e(k) &= \arctan(\Re[Q(k)]/\Im[Q(k)]) + n_\theta \\ &= \Delta\omega_d(k) + \phi(k-1) - \hat{\phi}(k-1) + v_\theta \end{aligned} \tag{3.29}$$

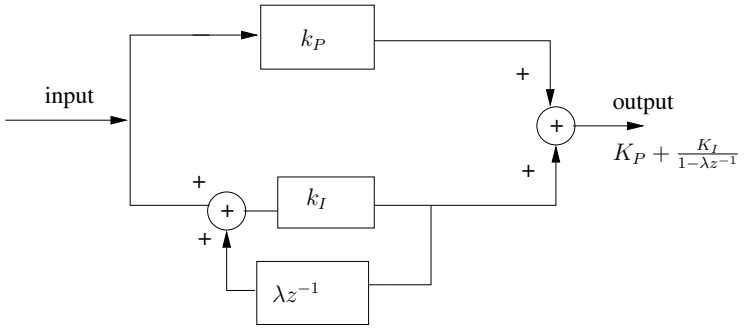

Figure 3.8: Block Diagram of PI Filter

where v_θ is the phase disturbance due to the input noise, and $\Delta\omega_d(k)+\phi(k-1)-\hat{\phi}(k-1)$ is the phase tracking error due to a noise-free incoming signal.

In the conventional method, the PI filter is selected as the loop filter. According to (3.29) and (3.16), our proposed method is that the Kalman filter will be the loop filter instead of the PI filter.

3.3 DDLL using Kalman Filter

We have introduced the mathmatical model of the DDLL and DPLL system in the previous section as shown in (3.16) and (3.29). In this section, we will introduce how to establish the state equation and the observation equation of the DDLL and DPLL system in the Kalman filter. As shown in Figure 3.9, in the DDLL system the state variable of the Kalman filter is $\rho(k)$, and the observation is $D(k,\rho,\delta)$. We assume that

$$\rho(k) = \xi(k) - \hat{\xi}(k) \tag{3.30}$$

We want to estimate the parameter $\rho(k)$ through the observation $D(k,\rho,\delta)$ by the Kalman filter. Once if we obtain the $\hat{\rho}(k|D(k,\rho,\delta))$, the parameter $\hat{\rho}(k|D(k,\rho,\delta))$ can be used to update the old parameter $\hat{\xi}(k)$. The equation is

$$\hat{\xi}(k+1) = \hat{\xi}(k) + \hat{\rho}(k|D(k,\rho,\delta)) \tag{3.31}$$

where $\hat{\xi}(k+1)$ is the new time delay estimate which the local oscillator uses to generate the next state local PRN code. The block diagram can be explained as shown in Figure

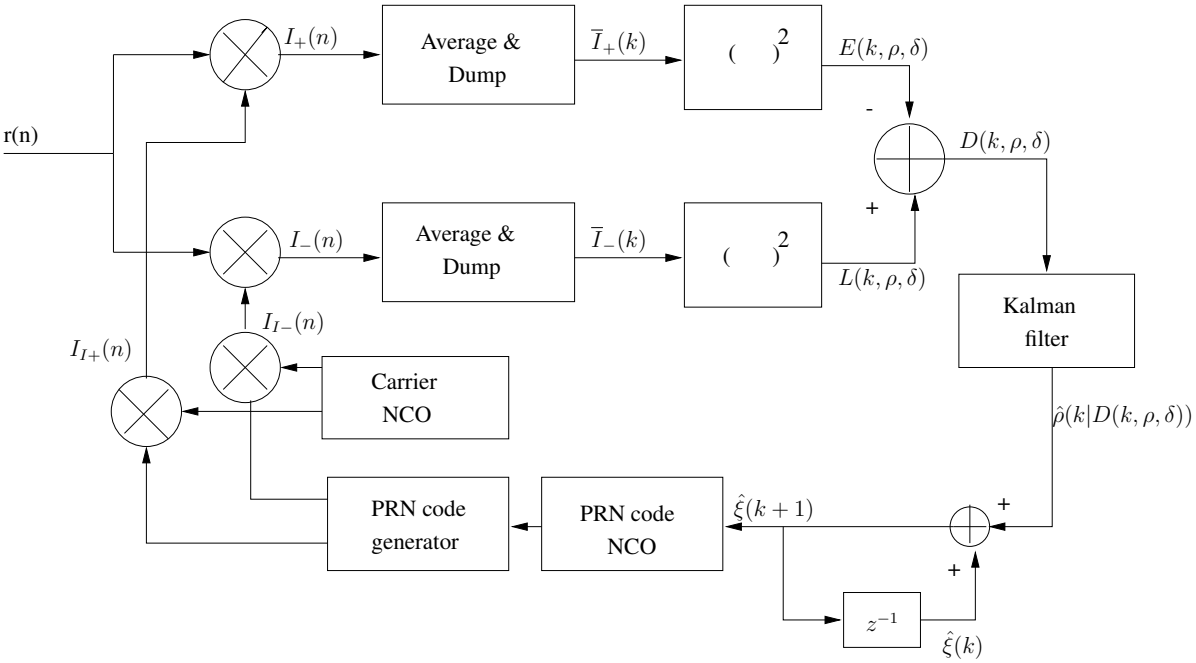

Figure 3.9: Block Diagram of the DDLL with Kalman Filter

3.9. The next state variable can be written as

$$\rho(k+1) = \xi(k+1) - \hat{\xi}(k+1) \tag{3.32}$$

According to the effect of the Doppler frequency on the time delay [3], the time delay $\xi(k+1)$ can be written as

$$\xi(k+1) = \xi(k) + \frac{f_d(k)}{f_L} \times \frac{(t_{k+1} - t_k)}{T_p} \tag{3.33}$$

Substituting (3.31) and (3.33) for (3.32), we can deduce that the state equation is

$$\rho(k+1) = \rho(k) + \frac{f_d(k)}{f_L} \times \frac{(t_{k+1} - t_k)}{T_p} - \hat{\rho}(k|D(k,\rho,\delta)) + v_\rho(k) \tag{3.34}$$

where $v_\rho(k)$ is the measurement noise and almost zero in our case.

The discriminator output function $D(k,\rho,\delta)$ is taken as the observation. The discriminator output function mentioned in (3.16) and (3.18) is rewritten as

$$\begin{aligned} D(k,\rho,\delta) &= L(k,\rho,\delta) - E(k,\rho,\delta) \triangleq K_0 D_\Delta(k,\rho,\delta) + v_D(k,\rho,\delta) \\ &= A^2 D^2(n) sinc^2[\Delta\omega_d(k)N/2][R^2(\rho(k)-\delta) - R^2(\rho(k)+\delta)] + v_D(k,\rho,\delta) \end{aligned} \tag{3.35}$$

Therefore, the state equation and observation equation of the Kalman filter in the DDLL system is written as

$$\rho(k+1) = \rho(k) + \frac{f_d(k)}{f_L} \times \frac{(t_{n+1} - t_n)}{T_p} - \hat{\rho}(k|D(k,\rho,\delta)) + v_\rho(k) \tag{3.36}$$

$$D(k,\rho,\delta) = A^2 D^2(n) sinc^2[\Delta\omega_d(k)N/2][R^2(\rho(k)-\delta) - R^2(\rho(k)+\delta)] + v_D(k,\rho,\delta) \tag{3.37}$$

where $\Delta\omega_d(k) = \omega_d(k) - \hat{\omega}_d(k)$.

According to (3.37), we can applying the mathmatical model to the Kalman filter. Because of the nonlinear observation equation, we must employ the extended Kalman filter (EKF) [7]. The EKF is to linearize the nonlinear state-space model at each time constant around the most recent state estimate. From (3.37) we know that the nonlinear measurement matrix $C(k,\rho(k))$ is

$$C(k,\rho(k)) = A^2 D^2(n) sinc^2[\Delta\omega_d(k)N/2][R^2(\rho(k)-\delta) - R^2(\rho(k)+\delta)] \tag{3.38}$$

and the partial derivative of the matrix $C(k,\rho(k))$ is written as

$$\begin{aligned} C(k) &= \frac{\partial C(k,\rho(k))}{\partial \rho(k)}\Big|_{\rho(k)=\hat{\rho}(k|D(k-1,\rho,\delta))} \\ &= A^2 D^2(n) sinc^2[\Delta\omega_d(k)N/2][2R(\hat{\rho}(k|D(k-1,\rho,\delta)) - \delta)R'(\hat{\rho}(k|D(k-1,\rho,\delta)) - \delta) \\ &\quad - 2R(\hat{\rho}(k|D(k-1,\rho,\delta)) + \delta)R'(\hat{\rho}(k|D(k-1,\rho,\delta)) + \delta)] \end{aligned} \tag{3.39}$$

where

$$R'(\hat{\rho}(k|D(k-1,\rho,\delta)) \pm \delta) = \frac{\partial R(\hat{\rho}(k|D(k-1,\rho,\delta)) \pm \delta)}{\partial \rho} \tag{3.40}$$

The linear transition matrix $F(k)$ from (3.37) is

$$F(k) = 1 \tag{3.41}$$

And then we can use the extended Kalman filter algorithm to compute state estimates recursively as shown in Figure 3.12. This leads to the following set of equations as shown in Table 3.1: $G_f(k)$ is referred to as the Kalman gain, and $K(k)$ is called as the error covariance.

Summary of the Extended Kalman Filter

Input vector process

observations:$D(1,\rho,\delta)$,$D(2,\rho,\delta)$,$D(3,\rho,\delta)$.....,$D(k,\rho,\delta)$

Known parameters

Nonlinear state transition matrix = $F(k)$

Nonlinear measurement matrix = $C(k,\rho(k))$

Correlation matrix of process noise vector $v_\rho(k)$ = $Q_1(n)$

Correlation matrix of measurement noise vector $v_D(k,\rho,\delta)$ = $Q_2(n)$

Computations : $k = 1, 2, 3..$

$$G_f(k) = K(k,k-1)H(k)[H(k)K(k,k-1)H(k) + Q_2(k)]^{-1}$$

$$\alpha(k) = \Psi(k) - H(k)\Delta\hat{\omega}_d(k|\Psi(k-1))$$

$$\Delta\hat{\omega}_d(k|\Psi(k)) = \Delta\hat{\omega}_d(k|\Psi(k-1)) + G_f(k)\alpha(k) - \Delta\hat{\omega}_d(k-1|\Psi(k-1))$$

$$\Delta\hat{\omega}_d(k+1|\Psi(k)) = \Phi(k)\Delta\hat{\omega}_d(k|\Psi(k))$$

$$K(k) = [I - G_f(k)H(k)]K(k,k-1)$$

$$K(k+1,k) = \Phi(k)K(k)\Phi(k) + Q_1(k)$$

Initial conditions

$$\hat{\rho}(1|D(0,\rho,\delta)) = E[\rho(1)]$$

$$K(1,0) = E[(\rho(1) - E[\rho(1)])(\rho(1) - E[\rho(1)])]$$

Table 3.1: DDLL using Kalman Filter

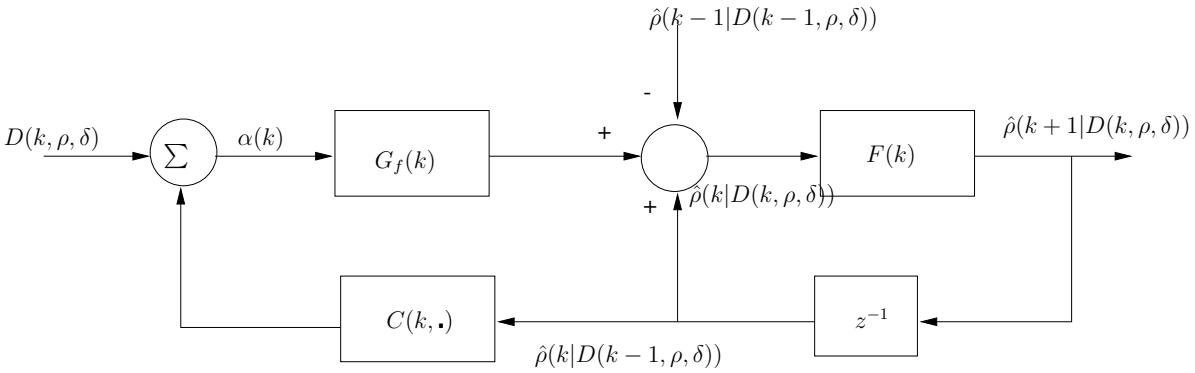

Figure 3.10: Block Diagram of the Kalman Filter in the DDLL system

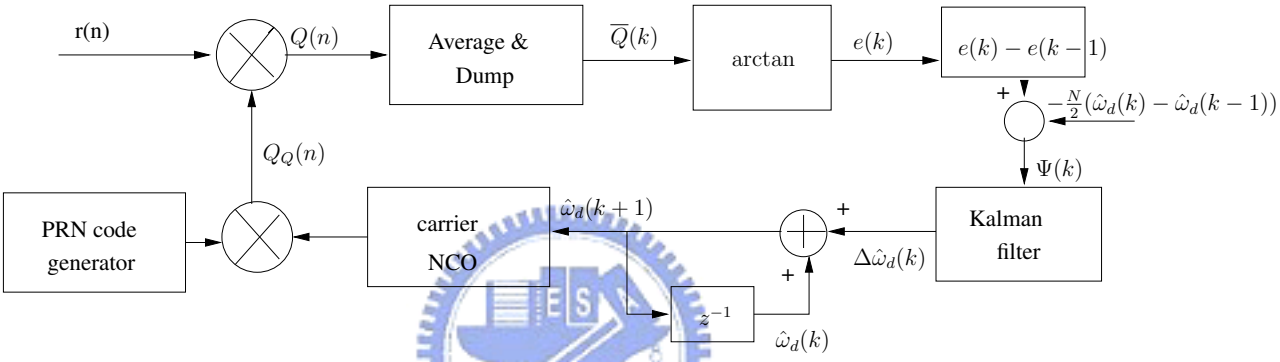

Figure 3.11: Block Diagram of the DPLL with Kalman Filter

3.4 DPLL using Kalman Filter

The block diagram of the DPLL system is shown in Figure 3.11. In the DPLL system the state variable of the Kalman filter is $\Delta\omega_d(k)$. The state variable $\Delta\omega_d(k)$ is defined as

$$\Delta\omega_d(k) = \omega_d(k) - \hat{\omega}_d(k) \tag{3.42}$$

Once if we obtain the $\Delta\hat{\omega}_d(k|\Psi(k))$, the parameter $\Delta\hat{\omega}_d(k|\Psi(k))$ can be used to update the previous parameter $\hat{\omega}_d(k)$. The equation is

$$\hat{\omega}_d(k+1) = \hat{\omega}_d(k) + \Delta\hat{\omega}_d(k|\Psi(k)) \tag{3.43}$$

And we will estimate the next state $\Delta\omega_d(k+1)$ when we receive the next input signal. The next state variable can be written as

$$\Delta\omega_d(k+1) = \omega_d(k+1) - \hat{\omega}_d(k+1) \tag{3.44}$$

Assume that $\omega_d(k+1)$ is unchanged in a short time, thus

$$\omega_d(k+1) = \omega_d(k) \tag{3.45}$$

Combining (3.43), (3.44) and (3.45), we can deduce that the state equation is

$$\begin{aligned}\Delta\omega_d(k+1) &= \omega_d(k) - \hat{\omega}_d(k) - \Delta\hat{\omega}_d(k|\Psi(k)) + v_{\Delta\omega_d}(k) \\ &= \Delta\omega_d(k) - \Delta\hat{\omega}_d(k|\Psi(k)) + v_{\Delta\omega_d}(k)\end{aligned} \tag{3.46}$$

where $v_{\Delta\omega_d}(k)$ is the measurement noise, and almost zero in our case. Because we want to estimate the Doppler frequency which is the rate of the phase change, we take the difference equation of (3.29) which is written as

$$\overline{\Psi}(k) = e(k) - e(k-1) \tag{3.47}$$

Substituting (3.26), (3.27), and (3.29) for (3.47), we can deduce that

$$\begin{aligned}\overline{\Psi}(k) &= (\omega_d(k) - \hat{\omega}_d(k)) \times \frac{N}{2} + (\omega_d(k) - \hat{\omega}_d(k-1)) \times \frac{N}{2} + v_\Psi(k) \\ &= \frac{N}{2}(2\Delta\omega_d(k) + \hat{\omega}_d(k) - \hat{\omega}_d(k-1)) + v_\Psi(k)\end{aligned} \tag{3.48}$$

where v_Ψ is the phase noise. Thus, if we want to obtain the observation equation, (3.48) minus $\frac{N}{2}(\hat{\omega}_d(k) - \hat{\omega}_d(k-1))$ is written as

$$\begin{aligned}\Psi(k) &= e(k) - e(k-1) - \frac{N}{2}(\hat{\omega}_d(k) - \hat{\omega}_d(k-1)) \\ &= \frac{N}{2}(2\Delta\omega_d(k) + \hat{\omega}_d(k) - \hat{\omega}_d(k-1)) - \frac{N}{2}(\hat{\omega}_d(k) - \hat{\omega}_d(k-1)) + v_\Psi(k) \\ &= N\Delta\omega_d(k) + v_\Psi(k)\end{aligned} \tag{3.49}$$

Therefore, we can conclude that the state and observation equation of the DPLL system in the Kalman filter can be written as

$$\Delta\omega_d(k+1) = \Delta\omega_d(k) - \Delta\hat{\omega}_d(k|\Psi(k)) + v_{\Delta\omega_d}(k) \tag{3.50}$$

$$\Psi(k) = N\Delta\omega_d(k) + v_\Psi(k) \tag{3.51}$$

According to (3.51), we can employ the Kalman Filter to estimate the parameter $\Delta\omega_d(k)$ in the linear state-space equation. The linear measurement matrix $H(k)$ from (3.51) is

$$H(k) = N \tag{3.52}$$

The linear transition matrix $\Phi(k)$ from (3.51) is

$$\Phi(k) = 1 \tag{3.53}$$

Therefore, we can compute the state estimates recursively by the Kalman filter algorithm as shown in Figure 3.12. This leads to the following set of equations as shown in Table 3.2. $G_f(k)$ is referred to as the Kalman gain, and $K(k)$ is called as the error covariance.

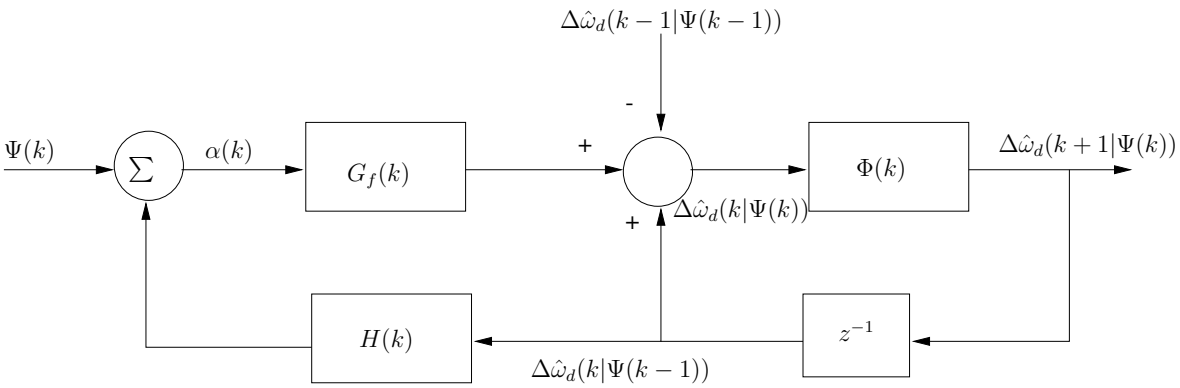

Figure 3.12: Block Diagram of the Kalman Filter in the DPLL system

Summary of the Kalman Filter

Input vector process

observations:$\Psi(1)$,$\Psi(2)$,$\Psi(3)$.....,$\Psi(k)$

Known parameters

Nonlinear state transition matrix = $\Phi(k)$

Nonlinear measurement matrix = $H(k)$

Correlation matrix of process noise vector $v_{\Delta\omega_d}(k)$ = $Q_1(n)$

Correlation matrix of measurement noise vector $v_{\Psi}(k)$ = $Q_2(n)$

Computations : $k = 1, 2, 3..$

$$G_f(k) = K(k, k-1)H(k)[H(k)K(k, k-1)H(k) + Q_2(k)]^{-1}$$

$$\alpha(k) = \Psi(k) - H(k)\Delta\hat{\omega}_d(k|\Psi(k-1))$$

$$\Delta\hat{\omega}_d(k|\Psi(k)) = \Delta\hat{\omega}_d(k|\Psi(k-1)) + G_f(k)\alpha(k) - \Delta\hat{\omega}_d(k-1|\Psi(k-1))$$

$$\Delta\hat{\omega}_d(k+1|\Psi(k)) = \Phi(k)\Delta\hat{\omega}_d(k|\Psi(k))$$

$$K(k) = [I - G_f(k)H(k)]K(k, k-1)$$

$$K(k+1, k) = \Phi(k)K(k)\Phi(k) + Q_1(k)$$

Initial conditions

$$\Delta\hat{\omega}_d(1|\Psi(0)) = E[\Delta\omega_d(1)]$$

$$K(1, 0) = E[(\Delta\omega_d(1) - E[\Delta\omega_d(1)])(\Delta\omega_d(1) - E[\Delta\omega_d(1)])]$$

Table 3.2: DPLL using Kalman Filter

Chapter 4

SIMULATIONS AND DISCUSSION

4.1 Simulation Environment

In this section, we establish our simulation environment. According to the characteristics of the real received signal, we use Matlab to simulate it. In the simulated received signal, the intermedia frequency is f_{IF}=3.996 MHz, the Doppler frequency f_d ranges from -10 kHz to 10 kHz, and the carrier frequency $f_c = f_{IF} + f_d$ ranges from 3.986 MHz to 4.006 MHz. The sampling frequency is f_s=6.138375 MHz, and the sampling time is $\frac{1}{f_s} = T_s$=162.9 ns. The code phase delay is set as $10T_s$. The signal-to-noise ratio, often written SNR, is a measure of signal strength relative to background noise. According to the actual condition of the global environment, the SNR is about -23 dB. In our simulation, the signal amplitude is 1, thus, the noise power is about 200. The simulated received signal looks like noise in Figure 4.1. The length of the correlation operation N is 6138 close to a C/A code chip time 1 ms or 3096 which about half of a C/A code chip time 0.5 ms. The acquisition loop must provide the coarse code delay and the initial Doppler frequency for the tracking loop before the tracking program is executed. Assume that the initial code delay error is within half of a code chip time, and the Doppler frequency error is within 200 Hz. So, we assume that the acquisition process provides the coarse code delay = $8T_s$. The parameter δ value is $3T_s$. The error covariance $K(k)$ value in the DDLL is 0.3, and in the DPLL is 0.03. The parameter λ is 0.99 of the PI filter as shown in Figure 3.8.

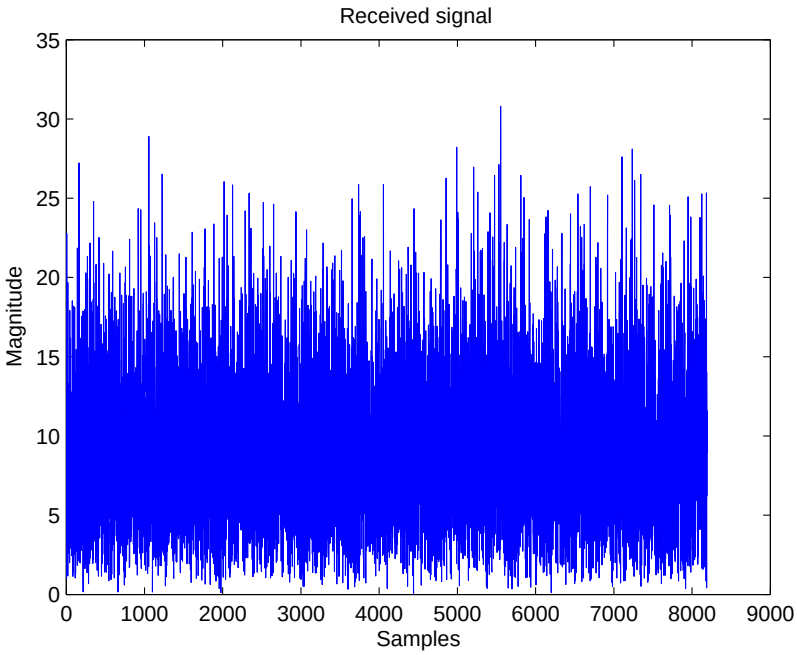

Figure 4.1: Received signal from the satellite 12 with SNR=-23 dB

4.2 Performance Measure

The mean function is expressed as

$$\mu_x(t) = \frac{1}{L}\sum_{i=1}^{L} x_i \tag{4.1}$$

where L is the total number of the tracking operation, and x_i is the estimated code delay or the estimated Doppler frequency. The standard deviation equation is

$$\sigma_x = [\frac{1}{L}\sum_{i=1}^{L}(x_i - \mu_x)^2]^{1/2} \tag{4.2}$$

where μ_x is the mean of the estimated code delay or the estimated Doppler frequency.

4.3 Simulation Results

In this section, we will show several examples to prove that our method is convenient to design. We have to try and error a lot of times in order to track all kinds of Doppler frequency, but if the Kalman filter is used, the tracking process design is achieved easily,

and the fine resolution of the estimated time delay and the Doppler frequency is obtained simply.

Example 1: Figure 4.2 and Figure 4.3 show that the resolution from the PI filter can be better than the resolution from the Kalman filter with the Doppler frequency 1 kHz, but the tracking speed in the Kalman filter is faster than it in the PI filter. Using the PI parameters of Figure 4.2 can not track the Doppler frequency 2 kHz as shown in Figure 4.4. But using Kalman filter can track any input signal with Doppler frequency from -5 kHz to 5 kHz obviously obtains a fine resolution without tuning any parameter value as shown in Figure 4.5 and 4.6. If we want to obtain more accurate resolution from the Kalman filter, we pass the Kalman filter output in Figure 4.5 to the low pass filter as shown in Figure 4.7 which shows that we get better resolution than using the PI filter by passing the Kalman filter output to a low pass filter.

Example 2: Figure 4.8 and 4.9 shows that the Doppler frequency changes with the maximum rate 0.000936 Hz/ms [2] using the PI filter and Kalman filter. Both of Figure 4.8 and 4.9 can find the fine Doppler frequency, and Figure 4.8 has the better resolution, but Figure 4.9 has the faster tracking speed. Figure 4.10 and 4.11 shows that if there is a frequency variation of the instant, the Kalman filter can track the input signal faster than the the PI iflter.

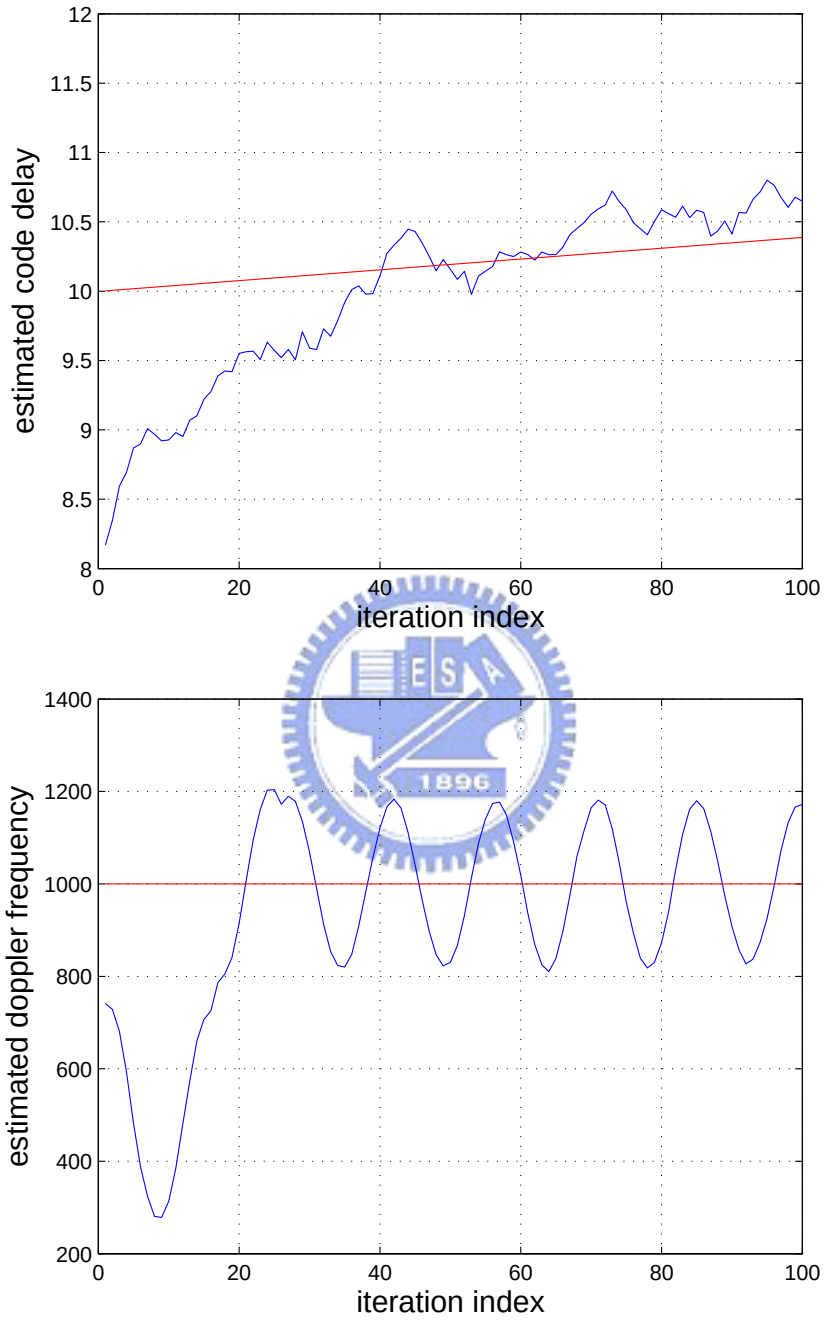

Figure 4.2: Using the PI filter with Doppler frequency 1 kHz, the estimated code delay variance = $0.1459T_s$, the estimated Doppler frequency variance = 37.6262 Hz, the convergence time = 40 ms

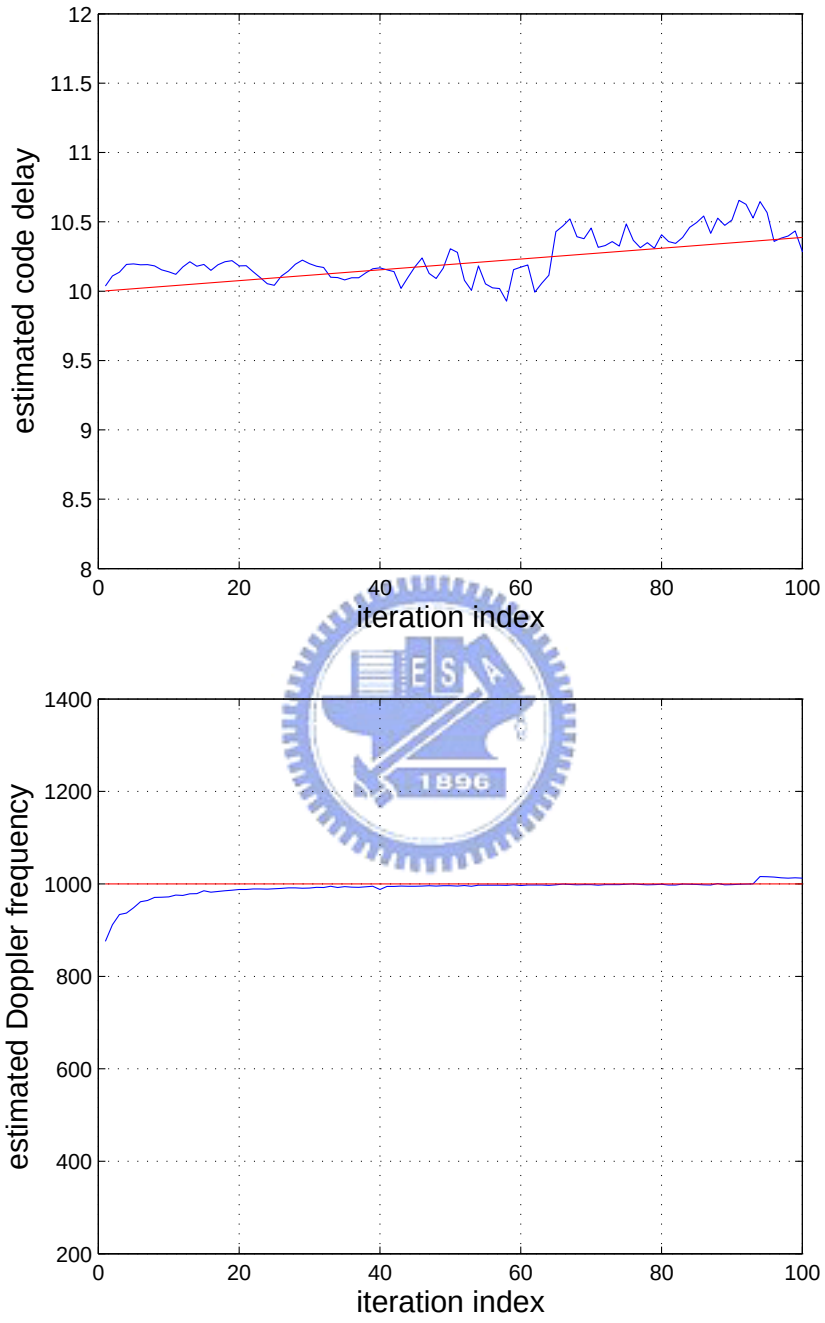

Figure 4.3: Using the Kalman filter with Doppler frequency 1 kHz, the estimated time delay variance = $0.199T_s$, the estimated Doppler frequency variance = 0.3902 Hz, the convergence time = 5 ms

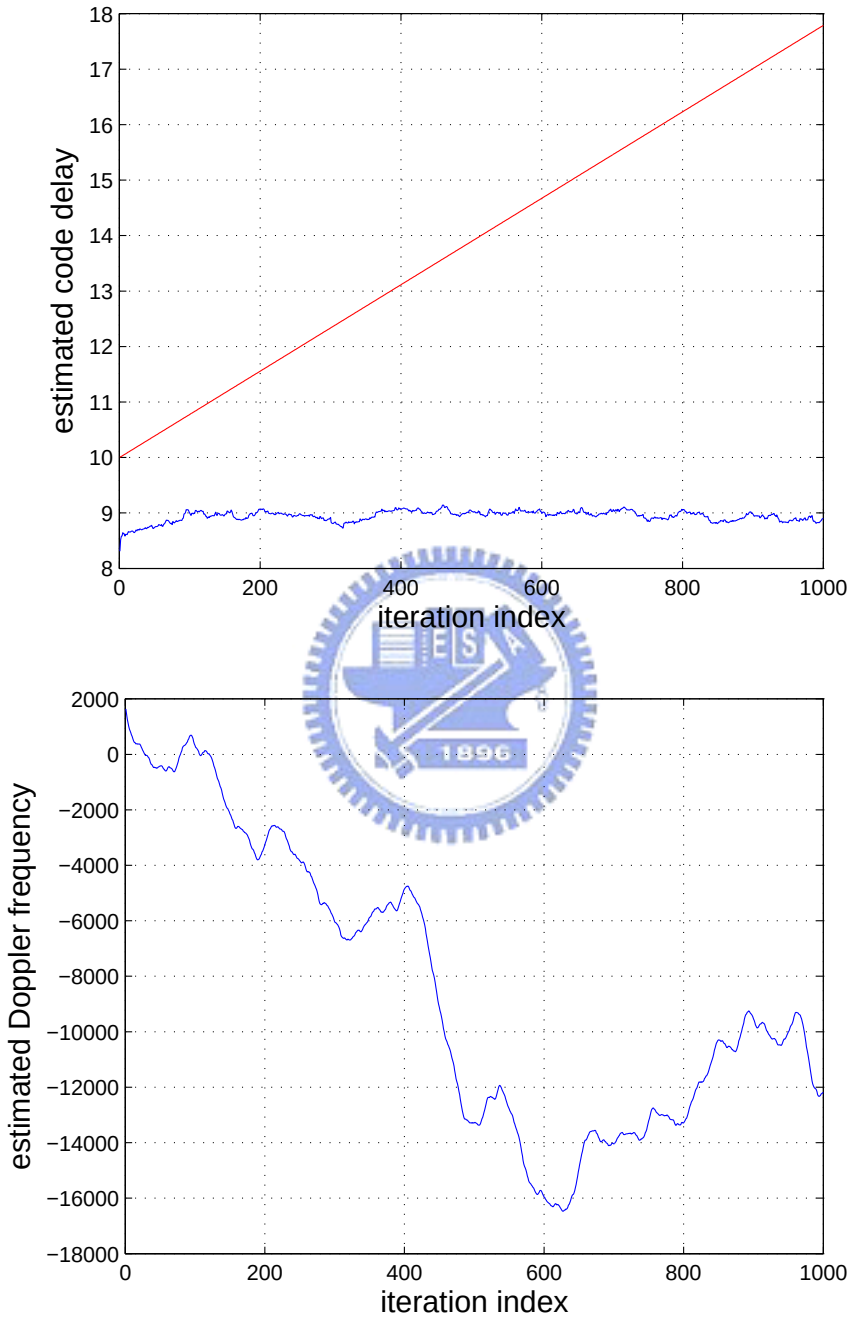

Figure 4.4: Using the PI filter without tracking the Doppler frequency 2 kHz of the PI parameters in the condition of Doppler frequency 1 kHz

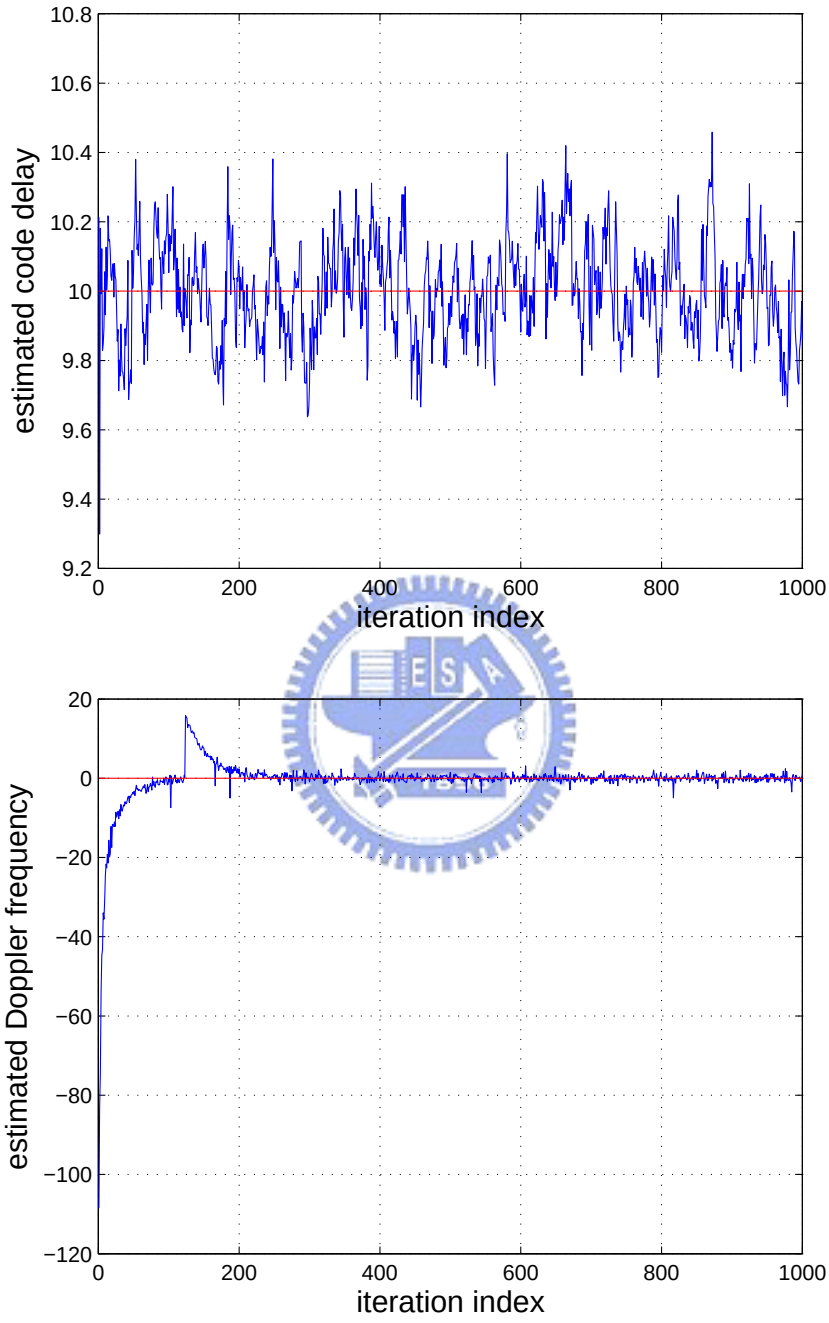

Figure 4.5: Using the Kalman filter with Doppler frequency 0 Hz, the estimated time delay variance = $0.1650T_s$, the estimated Doppler frequency variance = 0.2062 Hz, the convergence time = 5 ms

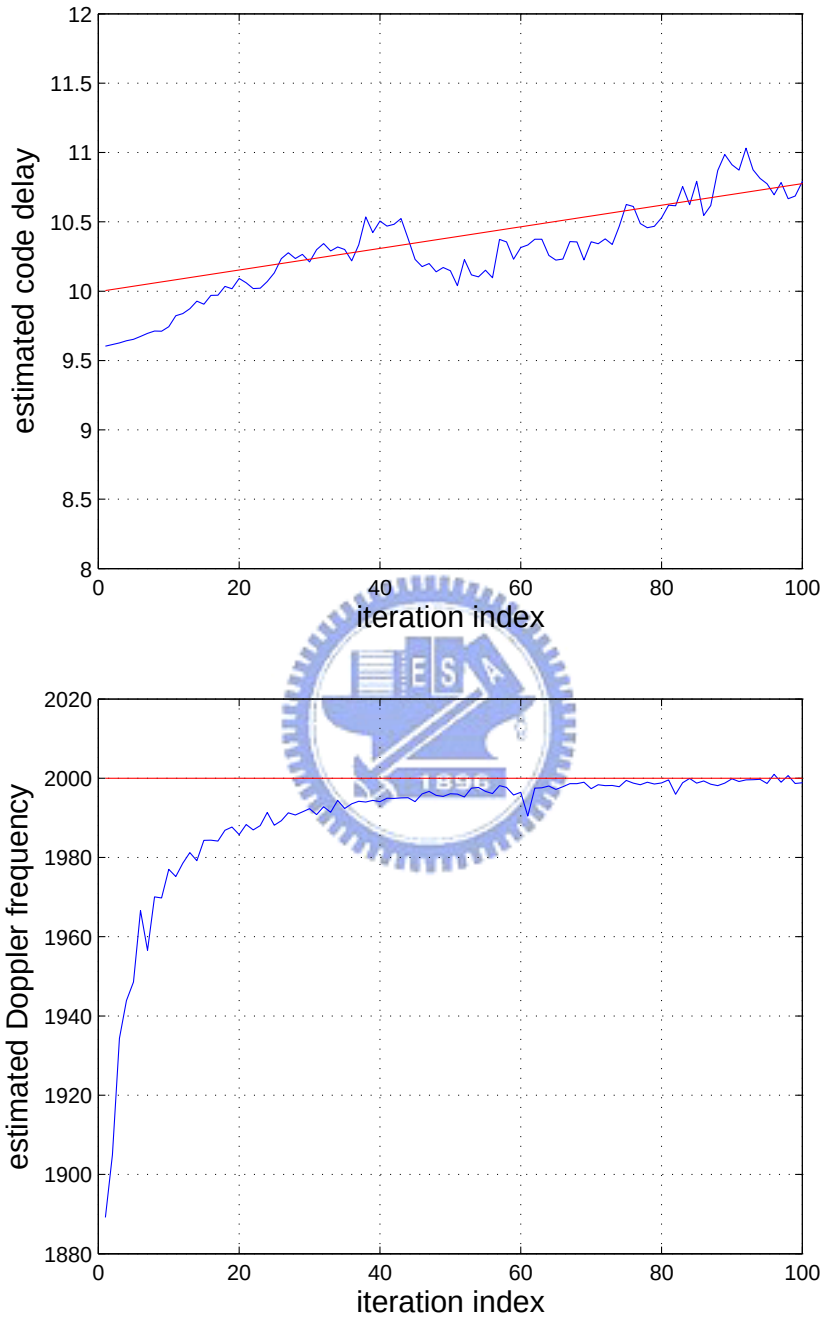

Figure 4.6: Using the Kalman filter with Doppler frequency 2 kHz, the estimated time delay variance = $0.2009T_s$, the estimated Doppler frequency variance = 0.0952 Hz, the convergence time = 50 ms

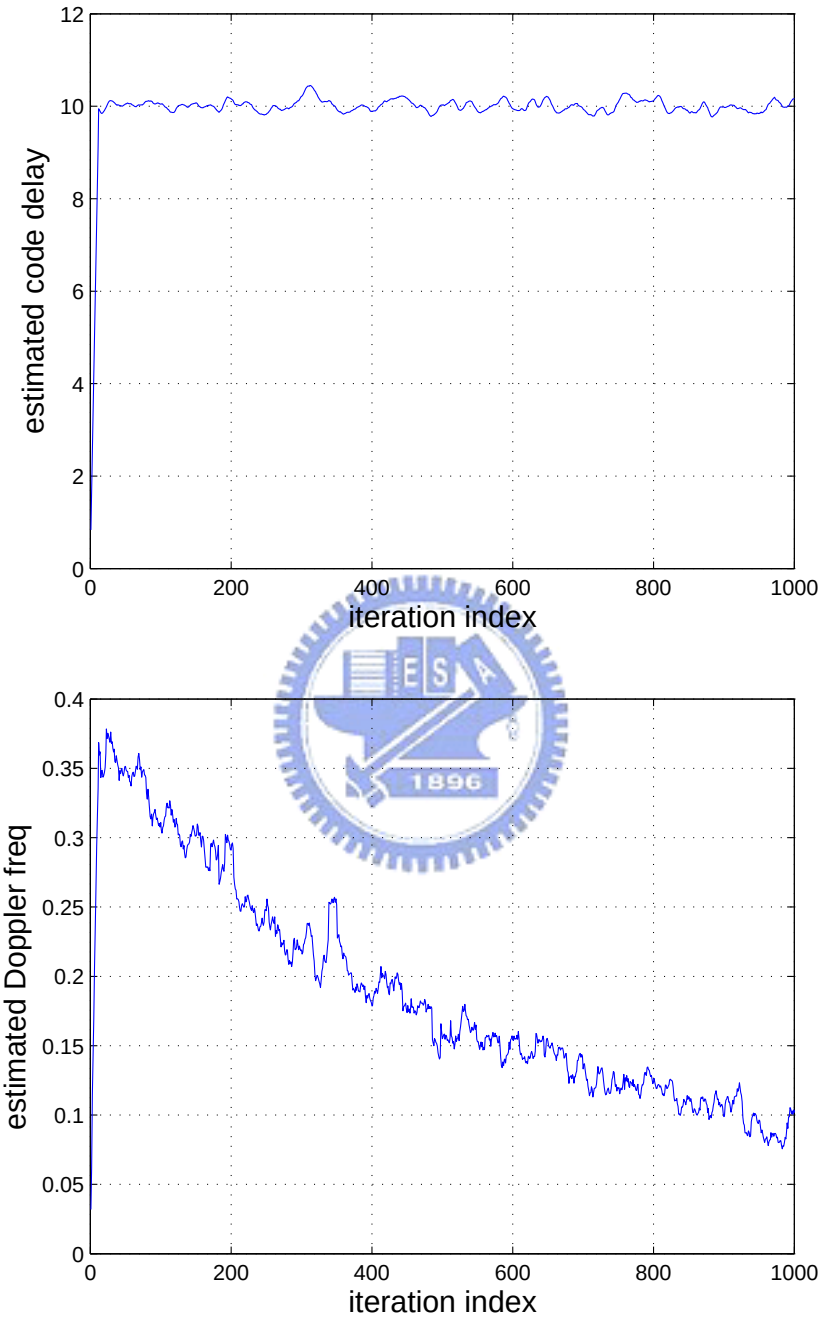

Figure 4.7: Using the Kalman filter with Doppler frequency 0 Hz, low-pass filter, the estimated time delay variance = $0.0057T_s$, the estimated Doppler frequency variance = 0.0019 Hz, the convergence time = 5 ms

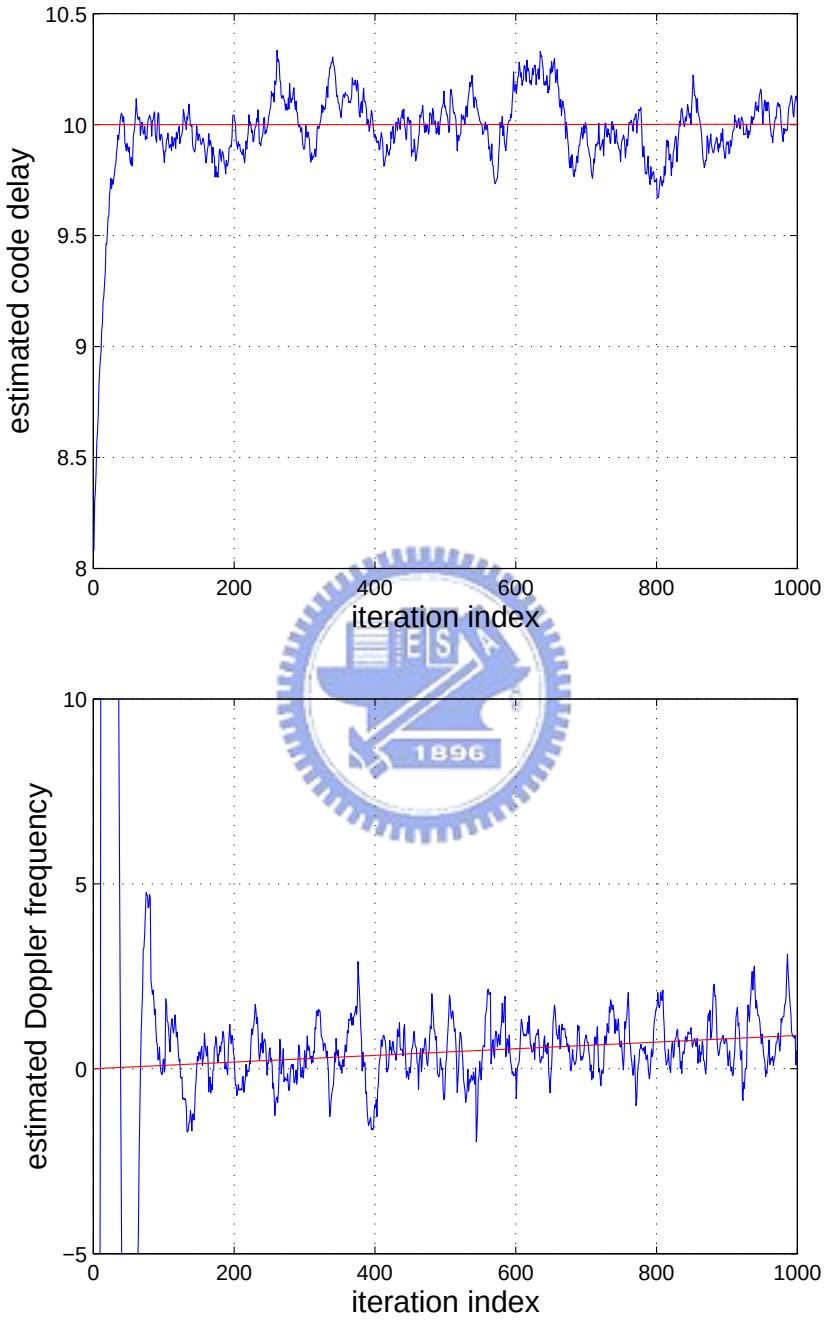

Figure 4.8: Using the PI filter with the estimated time delay variance = $0.1174T_s$, the estimated Doppler frequency variance = 0.2978 Hz

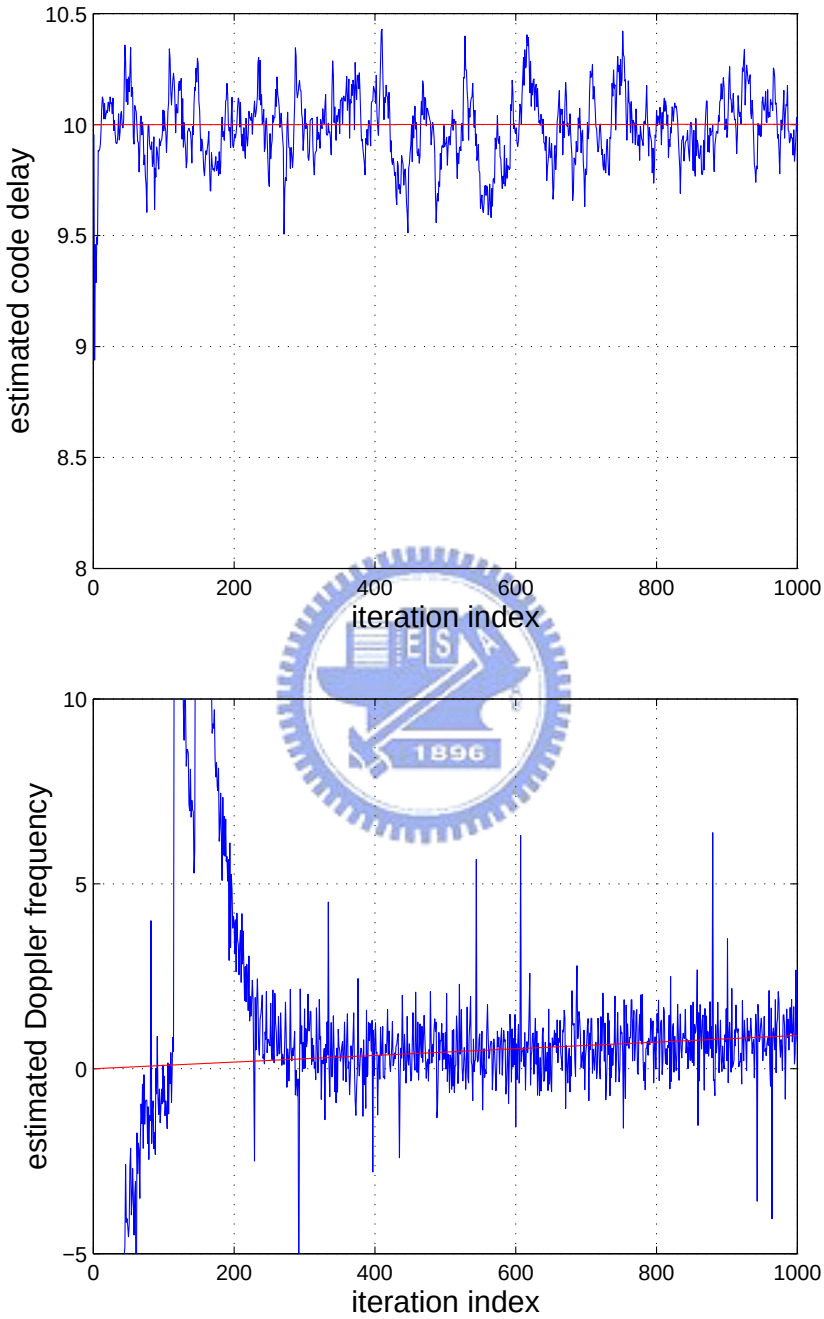

Figure 4.9: Using the Kalman filter with the estimated time delay variance = $0.1660T_s$, the estimated Doppler frequency variance = 3.0277 Hz

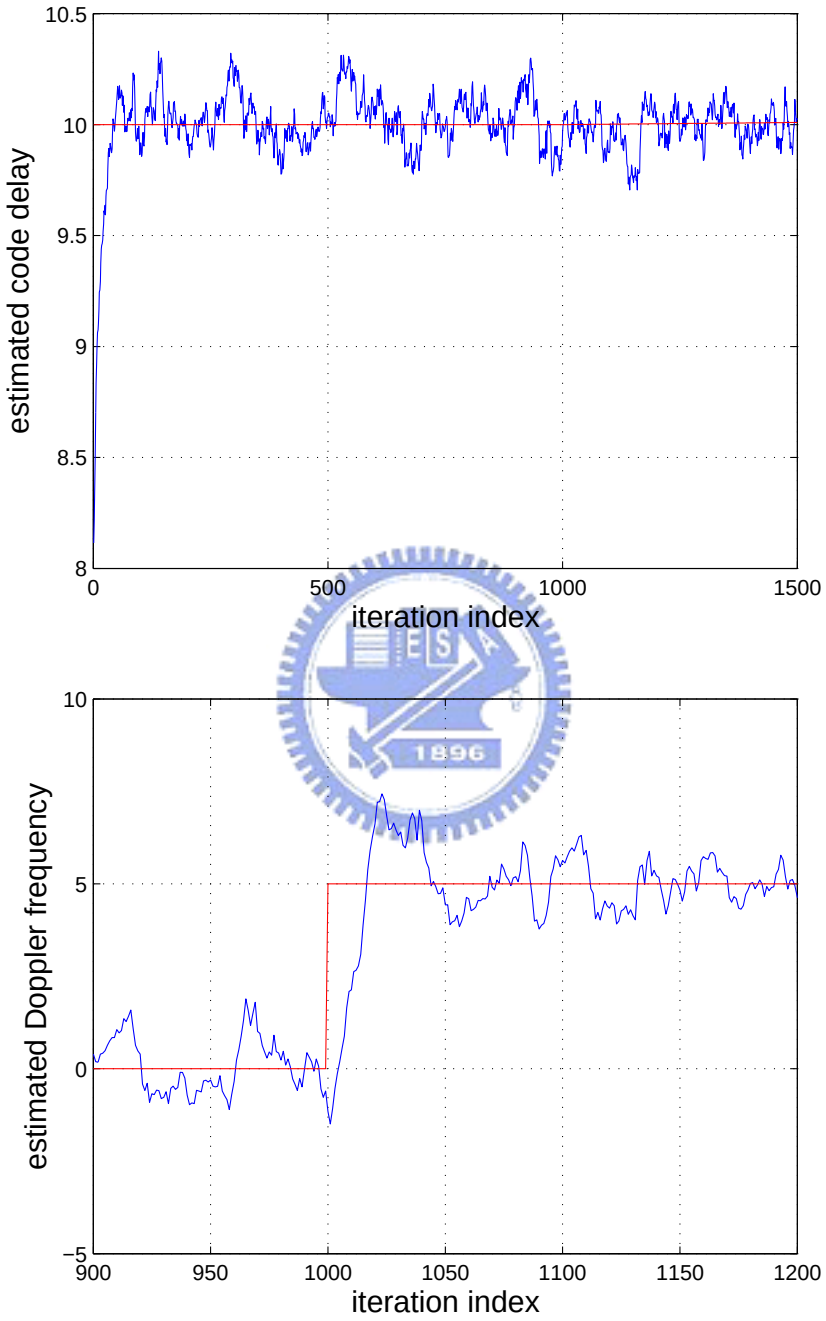

Figure 4.10: Using the PI filter with the estimated time delay variance = $0.1326T_s$, the estimated Doppler frequency variance = 0.6248 Hz

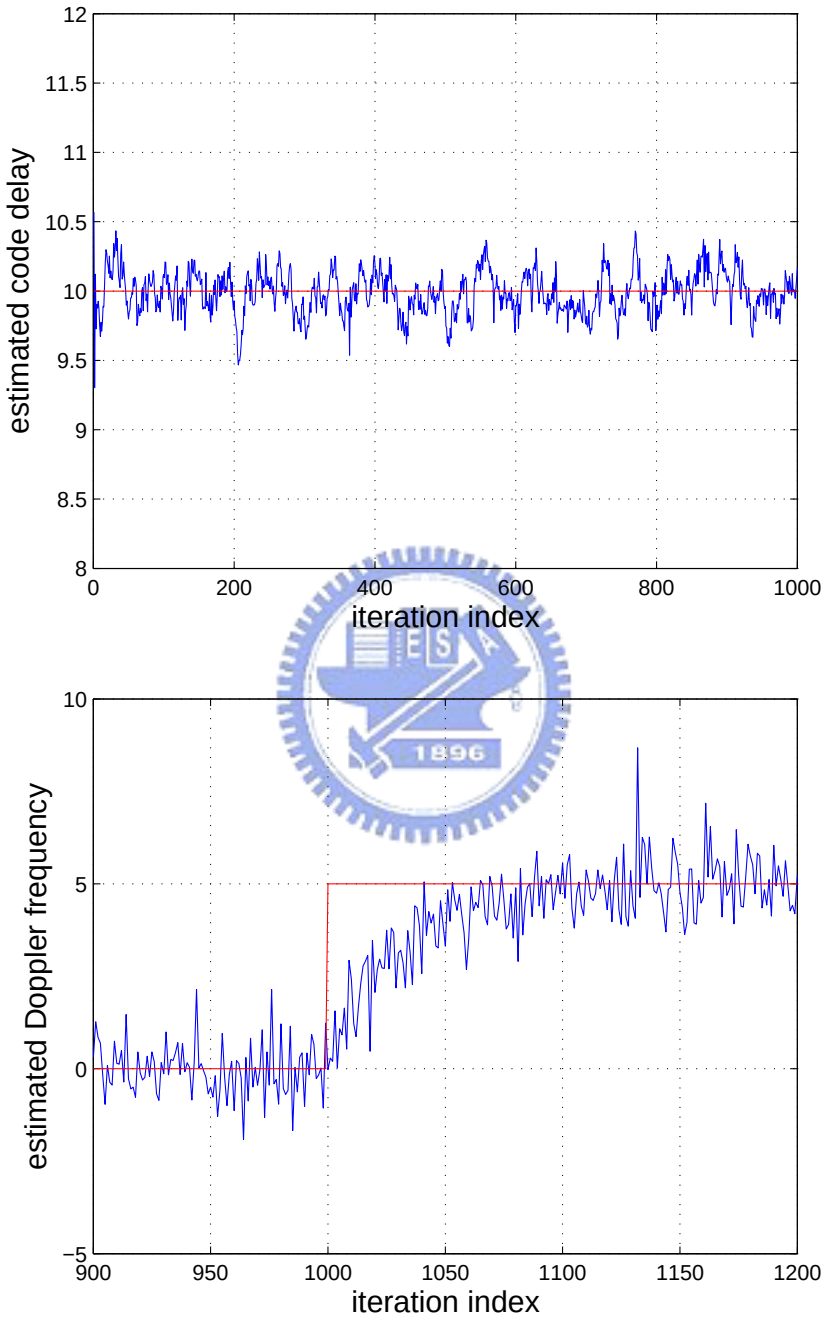

Figure 4.11: Using the Kalman filter with the estimated time delay variance = $0.1569T_s$, the estimated Doppler frequency variance = 3.0512 Hz

Chapter 5

CONCLUSIONS

In this thesis, the DPLL and DDLL system using Kalman filter algorithm is employed to develop an fast code delay and Doppler frequency tracking method in the GPS. Then, combining DPLL and DDLL system method is presented such that the tracking speed and design complexity can be reduced. Computer simulations demonstrate further that for GPS applications the proposed method performs satisfactorily with higher tracking speed and lower design complexity under the loop pull-in range. The proposed approach, naturally, is not limited to GPS applications, it can be applied to the tracking applications of any communications via the direct sequence spread spectrum.

Bibliography

[1] E. D. Kaplan, *Understanding GPS Principles and applications*, Artech. House. 1996.

[2] J. B.-Y. Tsui, *Fundamentals of Global Positioning System Receivers, A Software Approach*, Wiley, N. York, 2000.

[3] W. Zhuang, "Composite GPS receiver modeling, Simulations and Applications," Ph.D dissertation, Department of Electrical Engineering, University of New Brunswick, Fredericton, Oct. 1992.

[4] A.V. Oppenheim, R.W. Schafer, and J.R. Buck, *Discrete Time Signal Processing*, Prentice Hall International Editions, second edition, 1999.

[5] S. Haykin,*Communication Systems, 4th ed.* New York: Wiley, pp. 479- 509, 2000.

[6] J. L. Melsa and D. L. Cohn, *Decision and Estimation Theory*, McGraw Hill, 1978.

[7] S. S. Haykin, *Adaptive Filter Theory*, Englewood Cliffs, NJ: Prentice-Hall, 2nd ed., 1991.

[8] H. L. Van Trees, *Detection, Estimation, and Modulation Theory*, (Part I). New York: Wiley, 1968.

[9] "Global Positioning System Standard Positioning Service Signal Specification," 2nd ed., *GPS Joint Program Office*, Jan. 1995.

[10] N. Promkajin and S. Noppanakeepong, "An improvement to the adaptive kalman filter with the feedback of estimation error," *Student Conference on. Research and Development, 2003. SCORED 2003. Proceedings*, pp. 23- 28, 2003.

[11] C.C. Arcasoy and B. Koc, "Analytical Solution for Continuous-Time Kalman Tracking Filters with Colored Measurement Noise in Frequency Domain," *IEEE Trans. Aerospace and Electronic Systems*, Vol. 30, pp. 1059-1063, 1994.

[12] J.F. Wu, "A new fast frequency-acquisition technique using chirp transform algorithm for GPS receiver," M.S.thesis, Dept, of Electrical and Control Engineering, National Chiao Tung University, Hsinchu, Taiwan, R.O.C., July 2005.

[13] W.L. Mao, H.W. Tsao, and F.R. Chang, "A new fuzzy bandwidth carrier recovery system in GPS for robust phase tracking," *IEEE Signal Processing Letters*, Vol. 11, pp. 431-434 2004.

[14] S.J. Kim and R.A. Iltis, "STAP for GPS Receiver Synchronization," *IEEE Trans. Aerospace and Electronic Systems*, vol. 40, pp. 132-144, 2004.

[15] R. A. Iltis, "Joint estimation of PN code delay and multipath using the extended Kalman filter," *IEEE Trans. Commun.*, vol. 38, pp. 1677-1685, Oct. 1990.